

ITU-T

TELECOMMUNICATION
STANDARDIZATION SECTOR
OF ITU

G.650.2

(08/2015)

**SERIES G: TRANSMISSION SYSTEMS AND MEDIA,
DIGITAL SYSTEMS AND NETWORKS**

Transmission media and optical systems characteristics –
Optical fibre cables

**Definitions and test methods for statistical and
non-linear related attributes of single-mode fibre
and cable**

Recommendation ITU-T G.650.2

ITU-T G-SERIES RECOMMENDATIONS
TRANSMISSION SYSTEMS AND MEDIA, DIGITAL SYSTEMS AND NETWORKS

INTERNATIONAL TELEPHONE CONNECTIONS AND CIRCUITS	G.100–G.199
GENERAL CHARACTERISTICS COMMON TO ALL ANALOGUE CARRIER-TRANSMISSION SYSTEMS	G.200–G.299
INDIVIDUAL CHARACTERISTICS OF INTERNATIONAL CARRIER TELEPHONE SYSTEMS ON METALLIC LINES	G.300–G.399
GENERAL CHARACTERISTICS OF INTERNATIONAL CARRIER TELEPHONE SYSTEMS ON RADIO-RELAY OR SATELLITE LINKS AND INTERCONNECTION WITH METALLIC LINES	G.400–G.449
COORDINATION OF RADIOTELEPHONY AND LINE TELEPHONY	G.450–G.499
TRANSMISSION MEDIA AND OPTICAL SYSTEMS CHARACTERISTICS	G.600–G.699
General	G.600–G.609
Symmetric cable pairs	G.610–G.619
Land coaxial cable pairs	G.620–G.629
Submarine cables	G.630–G.639
Free space optical systems	G.640–G.649
Optical fibre cables	G.650–G.659
Characteristics of optical components and subsystems	G.660–G.679
Characteristics of optical systems	G.680–G.699
DIGITAL TERMINAL EQUIPMENTS	G.700–G.799
DIGITAL NETWORKS	G.800–G.899
DIGITAL SECTIONS AND DIGITAL LINE SYSTEM	G.900–G.999
MULTIMEDIA QUALITY OF SERVICE AND PERFORMANCE – GENERIC AND USER-RELATED ASPECTS	G.1000–G.1999
TRANSMISSION MEDIA CHARACTERISTICS	G.6000–G.6999
DATA OVER TRANSPORT – GENERIC ASPECTS	G.7000–G.7999
PACKET OVER TRANSPORT ASPECTS	G.8000–G.8999
ACCESS NETWORKS	G.9000–G.9999

For further details, please refer to the list of ITU-T Recommendations.

Recommendation ITU-T G.650.2

Definitions and test methods for statistical and non-linear related attributes of single-mode fibre and cable

Summary

Recommendation ITU-T G.650.2 contains definitions of the statistical and non-linear parameters of single-mode fibre and cable. It also contains both reference test methods and alternative test methods for characterizing these parameters.

This edition of the Recommendation has removed the state of polarization (SOP) method (first alternative test method).

History

Edition	Recommendation	Approval	Study Group	Unique ID*
1.0	ITU-T G.650	1993-03-12	XV	11.1002/1000/879
2.0	ITU-T G.650	1997-04-08	15	11.1002/1000/4017
3.0	ITU-T G.650	2000-10-06	15	11.1002/1000/5182
4.0	ITU-T G.650.1	2002-06-29	15	11.1002/1000/6072
4.0	ITU-T G.650.2	2002-06-29	15	11.1002/1000/6073
4.1	ITU-T G.650.1 (2002) Amd. 1	2003-03-16	15	11.1002/1000/6259
4.1	ITU-T G.650.2 (2002) Amd. 1	2003-03-16	15	11.1002/1000/6260
5.0	ITU-T G.650.1	2004-06-13	15	11.1002/1000/7319
5.0	ITU-T G.650.2	2005-01-13	15	11.1002/1000/7468
6.0	ITU-T G.650.2	2007-07-29	15	11.1002/1000/9152
6.0	ITU-T G.650.1	2010-07-29	15	11.1002/1000/10868
6.1	ITU-T G.650.1 (2010) Amd. 1	2012-10-29	15	11.1002/1000/11767
6.2	ITU-T G.650.1 (2010) Cor. 1	2013-08-29	15	11.1002/1000/11981
7.0	ITU-T G.650.2	2015-08-13	15	11.1002/1000/12528

* To access the Recommendation, type the URL <http://handle.itu.int/> in the address field of your web browser, followed by the Recommendation's unique ID. For example, <http://handle.itu.int/11.1002/1000/11830-en>.

FOREWORD

The International Telecommunication Union (ITU) is the United Nations specialized agency in the field of telecommunications, information and communication technologies (ICTs). The ITU Telecommunication Standardization Sector (ITU-T) is a permanent organ of ITU. ITU-T is responsible for studying technical, operating and tariff questions and issuing Recommendations on them with a view to standardizing telecommunications on a worldwide basis.

The World Telecommunication Standardization Assembly (WTSA), which meets every four years, establishes the topics for study by the ITU-T study groups which, in turn, produce Recommendations on these topics.

The approval of ITU-T Recommendations is covered by the procedure laid down in WTSA Resolution 1.

In some areas of information technology which fall within ITU-T's purview, the necessary standards are prepared on a collaborative basis with ISO and IEC.

NOTE

In this Recommendation, the expression "Administration" is used for conciseness to indicate both a telecommunication administration and a recognized operating agency.

Compliance with this Recommendation is voluntary. However, the Recommendation may contain certain mandatory provisions (to ensure, e.g., interoperability or applicability) and compliance with the Recommendation is achieved when all of these mandatory provisions are met. The words "shall" or some other obligatory language such as "must" and the negative equivalents are used to express requirements. The use of such words does not suggest that compliance with the Recommendation is required of any party.

INTELLECTUAL PROPERTY RIGHTS

ITU draws attention to the possibility that the practice or implementation of this Recommendation may involve the use of a claimed Intellectual Property Right. ITU takes no position concerning the evidence, validity or applicability of claimed Intellectual Property Rights, whether asserted by ITU members or others outside of the Recommendation development process.

As of the date of approval of this Recommendation, ITU had not received notice of intellectual property, protected by patents, which may be required to implement this Recommendation. However, implementers are cautioned that this may not represent the latest information and are therefore strongly urged to consult the TSB patent database at <http://www.itu.int/ITU-T/ipr/>.

© ITU 2015

All rights reserved. No part of this publication may be reproduced, by any means whatsoever, without the prior written permission of ITU.

Table of Contents

	Page
1 Scope.....	1
2 References.....	1
3 Terms and definitions	1
3.1 Polarization mode dispersion (PMD)	1
3.2 Types of test methods	7
4 Abbreviations and acronyms	7
5 Conventions	8
6 Test methods	8
6.1 Test methods for polarization mode dispersion.....	9
6.2 Test methods for non-linear attributes.....	35
Appendix I – Determination of PMD delay from an interferogram	36
I.1 RMS calculation for TINTY	36
I.2 RMS calculation for GINTY	38
Appendix II – Non-linear attributes	39
II.1 Background.....	39
II.2 Effective area (A_{eff}).....	39
II.3 Correction factor k.....	40
II.4 Non-linear coefficient (n_2/A_{eff})	42
II.5 Stimulated Brillouin scattering.....	43
II.6 Other effects	52
Appendix III – Test methods for effective area (A_{eff})	53
III.1 The far-field scan (FFS) technique	53
III.2 The variable aperture (VA) technique	55
III.3 The near-field scan (NFS) technique.....	59
Appendix IV – Information on polarization mode dispersion statistics	62
IV.1 Introduction	62
IV.2 Data collection.....	63
IV.3 Calculation of PMD_Q (Monte Carlo).....	63
IV.4 Calculation for DGD_{\max} (Monte Carlo).....	63
Bibliography.....	65

Recommendation ITU-T G.650.2

Definitions and test methods for statistical and non-linear related attributes of single-mode fibre and cable

1 Scope

This Recommendation contains definitions and test methods suitable mainly for factory measurements of the statistical and non-linear attributes of the single-mode optical fibres and cables described in [[b-ITU-T G.652](#)], [[b-ITU-T G.653](#)], [[b-ITU-T G.654](#)], [[b-ITU-T G.655](#)], [[b-ITU-T G.656](#)], and [[b-ITU-T G.657](#)]. These definitions and test methods are generally not appropriate for multimode fibre, such as that described in [[b-ITU-T G.651.1](#)]. Some of the test methods, when so indicated, may also be used to characterize discrete optical components, such as those described in [[b-ITU-T G.671](#)]. [[b-ITU-T G.650.1](#)] contains definitions and test methods for linear deterministic attributes.

Methods to compensate for impairments caused by polarization mode dispersion (PMD) can be found in [[b-ITU-T G.666](#)].

2 References

None.

3 Terms and definitions

This Recommendation defines the following terms (for more background information see [[b-IEC/TR 61282-9](#)]):

3.1 Polarization mode dispersion (PMD)

3.1.1 phenomenon of PMD: The differential group delay (DGD) time between two orthogonal polarized modes, which causes pulse spreading in digital systems and distortions in analogue systems.

NOTE 1 – In ideal circular symmetric fibres, the two polarization modes propagate with the same velocity. However, real fibres cannot be perfectly circular and can undergo local stresses; consequently, the propagating light is split into two local polarization modes travelling at different velocities. These asymmetry characteristics vary randomly along the fibre and in time, leading to a statistical behaviour of PMD. A "maximum" value of DGD can be inferred from the statistics.

NOTE 2 – For a given arbitrarily deployed fibre at a given time and optical frequency, there always exist two polarization states, called principal states of polarization (PSPs; see clause 3.1.2) such that the pulse spreading due to PMD vanishes if only one PSP is excited. Conversely, the maximum pulse spread due to PMD occurs when both PSPs are equally excited, and is related to the difference in the group delays associated with the two PSPs.

3.1.2 principal states of polarization (PSPs): When operating an optical fibre at a wavelength longer than the cut-off wavelength in a quasi-monochromatic regime, the output PSPs are the two orthogonal output states of polarization for which the output polarizations do not vary when the optical frequency is varied slightly. The corresponding orthogonal input polarization states are the input PSPs.

NOTE 1 – The local birefringence changes along the fibre, and the PSP depends on the fibre length (contrary to high-birefringence).

NOTE 2 – The PSPs are random complex vectors depending on time and optical frequency. However, according to the definition, there exists a small frequency range, the PSP bandwidth, over which they can be considered practically constant.

NOTE 3 – If a signal has a bandwidth broader than the PSP bandwidth, second order PMD effects come into play. They may imply a depolarization of the output field, together with an additional chromatic dispersion effect.

3.1.3 differential group delay (DGD; $[\Delta\tau(v)]$ in ps]):

The time difference in the group delays of the PSPs.

The DGD between two PSPs is wavelength-dependent and can vary randomly in time due to random mode coupling and randomized stresses along the optical propagation path due, among other causes, to environmental conditions. Variations in the order of a factor of two are typical for normal transmission fibres. As the PMD increases, the variance of the DGD values increases and the characteristic periodicity also decreases. For normal random-mode-coupled fibre, the DGD distribution is ergodic, which means that the distribution remains the same over time and wavelength, for a sufficiently long period or wide range. This allows an assumption that measurements over a finite wavelength range are representative of other wavelength ranges or the same wavelength range at different times over a long period of time. For mode-coupled fibres, the distribution is usually Maxwellian.

Instantaneous DGD values limit the transmission capacity of digital systems. The derivative of the DGD with respect to the wavelength limits the signal-to-noise ratio (SNR) in analogue systems. Therefore, the statistical distribution of the DGDs (vs time or vs wavelength) plays an important role in predicting real system performance.

Negligible mode coupling is found on some specialty fibre, such as polarization-maintaining fibre (PMF), and some components. For these devices, there is very little DGD variation with wavelength.

The DGD is measured in picoseconds.

3.1.4 PMD value:

PMD_{Avg} is defined as the linear average $\langle \Delta\tau \rangle$ of the DGD values $\Delta\tau(v)$ over a given optical frequency range v_1 to v_2 ,

$$\text{PMD}_{\text{Avg}} = \langle \Delta\tau \rangle = \frac{\int_{v_1}^{v_2} \Delta\tau(v) dv}{v_2 - v_1} \quad (3-1)$$

PMD_{RMS} is defined as the root mean square (RMS) $\langle \Delta\tau^2 \rangle^{1/2}$ of the DGD values $\Delta\tau(v)$ over a given optical frequency range v_1 to v_2 ,

$$\text{PMD}_{\text{RMS}} = \langle \Delta\tau^2 \rangle^{1/2} = \left(\frac{\int_{v_1}^{v_2} \Delta\tau(v)^2 dv}{v_2 - v_1} \right)^{1/2} \quad (3-2)$$

NOTE 1 – For Equations 3-1 and 3-2 to be valid, the range v_1 to v_2 should be sufficiently wide, e.g., of the order of 100 nm in the corresponding wavelength range.

If the distribution of these DGD values over the given optical frequency range may be approximated by a Maxwell distribution with sufficient amount of confidence and fidelity, PMD_{Avg} can be mathematically related to PMD_{RMS}.

$$\langle \Delta\tau \rangle = \left(\frac{8}{3\pi} \right)^{1/2} \langle \Delta\tau^2 \rangle^{1/2} \quad (3-3)$$

For fibre and cable, the PMD reference test method (RTM) reports the linear average.

NOTE 2 – Averaging over temperature, time or mechanical perturbations is generally an acceptable alternative to averaging over frequency. In this case, the expected value operator is over all conditions. The expected value of a set of finite wavelengths at a given time is equal to the long-term expected value over any frequency range. Both Equations 3-1 and 3-2 are considered as an averaging in this context.

NOTE 3 – Equation 3-3 applies only when the distribution of DGDs is Maxwellian, for instance, when the fibre is randomly mode coupled. The generalized use of Equation 3-3 can be verified by statistical analysis. A Maxwell distribution may not be the case if there are point sources of elevated birefringence (relative to the rest of the fibre), such as a tight bend, or other phenomena that reduce the mode coupling, such as a continual reduced bend radius with fibre in tension. In these cases, the distribution of the DGDs will begin to resemble the square root of a non-central Chi-square distribution with three degrees of freedom. For these cases, the PMD_{RMS} value will generally be larger relative to the PMD_{Avg} that is indicated in Equation 3-3.

3.1.5 PMD coefficient:

The PMD value normalized to the measurement length.

There are two normalization formulas, one for random mode coupling, associated with normal transmission fibres, and one for negligible mode coupling, associated with specialty fibres such as polarization maintaining fibres.

3.1.5.1 random mode coupling: For random mode coupling, the PMD coefficient is the PMD value (PMD_{Avg} or PMD_{RMS}) divided by the square root of the length ($L^{1/2}$) and is usually reported in picoseconds per root kilometre.

3.1.5.2 negligible mode coupling: For negligible mode coupling, the PMD coefficient is the PMD value (PMD_{Avg} or PMD_{RMS}) divided by the length (L) and may be reported in picoseconds per kilometre or femtoseconds per metre.

3.1.6 mathematical definitions: PMD can be described in terms of Stokes or Jones vectors. The evolution of the output Jones vector with angular optical frequency, $\omega = 2\pi\nu = 2\pi c/\lambda$, is the source of system impairment. All parameters, vectors and matrices in the following are functions of angular optical frequency.

For the following considerations it is assumed that the signal is fully polarized and that polarization dependent loss (PDL) is negligible.

The normalized Jones vector \vec{j} , with complex elements, j_x and j_y , is defined as:

$$\vec{j} = \begin{bmatrix} \cos \theta \exp(-i\mu/2) \\ \sin \theta \exp(i\mu/2) \end{bmatrix} \quad (3-4)$$

where:

θ is the linear orientation of the Jones vector

μ is the phase separation of the two elements of the Jones vector

i is $\sqrt{-1}$, the imaginary unit

The normalized Stokes vector \vec{s} in Cartesian coordinates, usually numbered 1, 2, 3, is defined as:

$$\vec{s} = \begin{bmatrix} |j_x|^2 - |j_y|^2 \\ 2 \operatorname{Re} \{ j_x j_y^* \} \\ -2 \operatorname{Im} \{ j_x j_y^* \} \end{bmatrix} = \begin{bmatrix} \cos 2\theta \\ \sin 2\theta \cos \mu \\ \sin 2\theta \sin \mu \end{bmatrix} \quad (3-5)$$

where:

$|j_x|^2 = j_x^* j_x$ is the squared magnitude of j_x

j_y^* is the complex conjugate of j_y .

NOTE 1 – The minus sign for s_3 in (Equation 3-5) does result in Stokes vector rotations following the right hand rule. It does not affect the DGD measurements.

Cartesian coordinates s_1 , s_2 and s_3 can be related to spherical coordinates ψ and χ as follows:

$$\begin{bmatrix} s_1 \\ s_2 \\ s_3 \end{bmatrix} = \begin{bmatrix} \cos \psi \cos \chi \\ \sin \psi \cos \chi \\ \sin \chi \end{bmatrix} \quad (3-6)$$

and, inversely,

$$\tan \psi = \frac{s_2}{s_1} \quad (3-7)$$

$$\sin \chi = s_3 \quad (3-8)$$

where:

ψ is the longitude

χ is the latitude

NOTE 2 – Sometimes χ is defined as $\pi/2 - \chi$. In this case, $\sin \chi$ must be replaced by $\cos \chi$.

From Equations 3-5 to 3-8, the Stokes vector in spherical coordinates ψ and χ can be calculated as a function of θ and μ :

$$\tan \psi = \tan 2\theta \cos \mu \quad (3-9)$$

$$\sin \chi = \sin 2\theta \sin \mu \quad (3-10)$$

For a given frequency, ω_0 , the relationship between the input Stokes vector, \vec{s}_0 , to output vector can be described as a three-dimensional real rotation matrix, R , with rotation angle, γ_{ROT} , and rotation vector, \vec{y} .

$$\vec{s} = R\vec{s}_0 \text{ where } R = \vec{y}\vec{y}^T(1 - \cos \gamma_{ROT}) + I \cos \gamma_{ROT} + [\vec{y} \times] \sin \gamma_{ROT} \quad (3-11)$$

the rotation vector \vec{y} is a column vector, consequently, \vec{y}^T is a row vector and

$$\vec{y}\vec{y}^T = \begin{bmatrix} y_1^2 & y_1y_2 & y_1y_3 \\ y_1y_2 & y_2^2 & y_2y_3 \\ y_1y_3 & y_2y_3 & y_3^2 \end{bmatrix} \text{ is a matrix, } I \text{ is the identity matrix and}$$

$$[\vec{y} \times] = \begin{bmatrix} 0 & -y_3 & y_2 \\ y_3 & 0 & -y_1 \\ -y_2 & y_1 & 0 \end{bmatrix} \text{ is the cross-product operator.}$$

At this frequency, the relationship of the output Jones vector to input vector, \vec{j}_0 , is given by the matrix, T , as:

$$\vec{j} = T\vec{j}_0 \quad \text{where } T = \begin{bmatrix} \cos \gamma_T - iy_1 \sin \gamma_T & -\sin \gamma_T (y_3 + iy_2) \\ \sin \gamma_T (y_3 - iy_2) & \cos \gamma_T + iy_1 \sin \gamma_T \end{bmatrix} \quad (3-12)$$

$\gamma_{ROT} = 2\gamma_T$ and the subscripted values are the elements of the rotation vector.

The polarization dispersion vector (PDV), $\vec{\Omega}$, is used to describe the variation of the output vectors with frequency. In the Stokes notation, it is defined as:

$$\frac{d\vec{s}(\omega)}{d\omega}\Big|_{\omega_0} = \frac{dR(\omega)}{d\omega}\Big|_{\omega_0} R^T(\omega_0) \vec{s}(\omega_0) = \vec{\Omega} \times \vec{s}(\omega_0) \quad (3-13)$$

In the Jones notation, it is defined as follows, where the subscripted values are the elements of the PDV:

$$\frac{d\vec{j}(\omega)}{d\omega}\Big|_{\omega_0} = \frac{dT(\omega)}{d\omega}\Big|_{\omega_0} T \times (\omega_0) \vec{j}(\omega_0) = -\frac{i}{2} \begin{bmatrix} \Omega_1 & \Omega_2 - i\Omega_3 \\ \Omega_2 + i\Omega_3 & -\Omega_1 \end{bmatrix} \vec{j}(\omega_0) \quad (3-14)$$

Equation 3-14 can be used as the basis of a first order Taylor expansion for the evolution of the output Jones vector in the neighbourhood of ω_0 .

The PDV can be related to the PSP, \vec{p} , and DGD, $\Delta\tau$, as well as the rotation vector and angle as:

$$\vec{\Omega} = 2 \frac{d\gamma_T}{d\omega} \vec{y} + \sin 2\gamma_T \frac{d\vec{y}}{d\omega} + 2 \sin^2 \gamma_T \left(\vec{y} \times \frac{d\vec{y}}{d\omega} \right) = \Delta\tau \vec{p} \quad (3-15)$$

Equation 3-14 can be written as:

$$\frac{d\vec{j}(\omega)}{d\omega}\Big|_{\omega_0} = \frac{dT(\omega)}{d\omega}\Big|_{\omega_0} T \times (\omega_0) \vec{j}(\omega_0) = -\frac{i}{2} \Delta\tau V_p \begin{bmatrix} 1 & 0 \\ 0 & -1 \end{bmatrix} V \times \vec{j}(\omega_0) \quad (3-16)$$

where:

$$V_p = \begin{bmatrix} \cos \theta_p \exp(-i\mu_p/2) & -\sin \theta_p \exp(-i\mu_p/2) \\ \sin \theta_p \exp(i\mu_p/2) & \cos \theta_p \exp(i\mu_p/2) \end{bmatrix}$$

V_p^* is the transpose conjugate of V_p

$$\text{and the PSP is } \vec{p} = \begin{bmatrix} \cos 2\theta_p \\ \sin 2\theta_p \cos \mu_p \\ \sin 2\theta_p \sin \mu_p \end{bmatrix}$$

Assuming that the PSPs are frequency invariant (over a narrow frequency interval, ω_0 and $\omega_0 + \Delta\omega$), Equation 3-14 has a solution in the neighbourhood of ω_0 :

$$\hat{j}(\varpi) = V_p \begin{bmatrix} \exp[-i\varpi\Delta\tau/2] & 0 \\ 0 & \exp[i\varpi\Delta\tau/2] \end{bmatrix} V_p \times \vec{j}(\omega_0) = J(\varpi) \vec{j}(\omega_0) \quad (3-17)$$

where ϖ is the deviation from ω_0 .

In the Stokes notation, Equation 3-17 corresponds to a rotation of $\varpi\Delta\tau$ about the PSP on the Poincaré sphere (PS).

Equation 3-17 is written as a singular value decomposition. The diagonal elements of the central matrix are the eigenvalues. The columns of the matrix, V_p , are the eigenvectors, which are in the Jones vector form. The first column converts to the PSP in the same form as in Equation 3-5. Call this \hat{j}_p . This matrix can also be expressed in the form of Equation 3-12, with $\varpi\Delta\tau/2$ replacing γ_T and with the elements of the PSP replacing the elements of the rotation vector.

A change of coordinates can be applied to Equation 3-17 so the PSP matrix in the new coordinate system is the identity matrix. The x and y elements of the result can be convolved with the frequency domain field of a monochromatic source which can then be expressed in the time domain as a power

function. For example, a Gaussian temporal pulse with RMS width equal to σ , in picoseconds, and a fibre with chromatic dispersion, D , in picoseconds per nanometre). The resultant output power function is a split pulse, $P(t)$:

$$P(t) = \frac{1}{S\sqrt{2\pi}} \left\{ \exp\left[-\frac{(t - (\tau_G - \Delta\tau/2))^2}{2S^2}\right] u + \exp\left[-\frac{(t - (\tau_G + \Delta\tau/2))^2}{2S^2}\right] (1-u) \right\} \quad (3-18)$$

where τ_G is the group delay for $u = 0.5$

$$S^2 = \sigma^2 + \left(\frac{\tau'}{2\sigma}\right)^2 \text{ and } \tau' = -D \frac{\lambda_0}{\omega_0}$$

$$u = [\vec{j}_p \times T(\omega_0) \vec{j}_0] \times [\vec{j}_p \times T(\omega_0) \vec{j}_0] \text{ in the original coordinates.}$$

The difference between pulse centre for $u = 0$ is $\Delta\tau$ away from the pulse centre for $u = 1$. This is the meaning of DGD. These values of u are achieved when the output Jones vector is aligned with \vec{j}_p or its orthogonal counterpart, the other eigenvector.

The RMS width of this pulse is:

$$\text{RMS}_p = [S^2 + \Delta\tau^2 u(1-u)]^{1/2} \quad (3-19)$$

In measurements using the RTM Jones matrix eigenanalysis (JME), estimates of the T matrix are calculated for ω_0 and $\omega_0 + \Delta\omega$, a frequency slightly larger. The frequency transfer matrix is approximated as:

$$J(\Delta\omega) = T(\omega_0 + \Delta\omega)T^{-1}(\omega_0) \quad (3-20)$$

It is clear from Equation 3-17 that the argument of the ratio of eigenvalues, divided by $\Delta\omega$, is the DGD.

The term "first order" was originally associated with the first-order Taylor expansion associated with Equation 3-14. It could also be associated with the fact that it provides a continuous phase-linear map from the Jones vector at one frequency to the next higher frequency.

Second order PMD could be thought of as a description of $J(\varpi)$ that provides a continuous mapping to both the frequency above and the frequency below. This can be done by replacing $\varpi\Delta\tau/2$ by a more general expression, $\gamma(\varpi)$, that is described as a Taylor expansion:

$$\gamma(\varpi) = \varpi\gamma_{\varpi} + \varpi^2\gamma'_{\varpi}/2 \quad (3-21)$$

Similarly, the angular parameters of the PSP can be written as:

$$\theta_p(\varpi) = \theta_{p0} + \varpi\theta_{p\varpi} \quad \text{and} \quad \mu_p(\varpi) = \mu_{p0} + \varpi\mu_{p\varpi} \quad (3-22)$$

The use of formulae such as Equation 3-20 for the reverse frequency, the singular value decomposition of Equation 3-17, and some algebra/trigonometry can yield estimates of the parameters of Equations 3-21 and 3-22 from measured data.

The second order PDV, $\vec{\Omega}_{\varpi}$, is defined as the frequency derivative of the PDV:

$$\vec{\Omega}_{\varpi} = \frac{d\vec{\Omega}}{d\varpi} = \frac{d\Delta\tau}{d\varpi} \vec{p} + \Delta\tau \frac{d\vec{p}}{d\varpi} \quad (3-23)$$

When random mode coupling is present, the magnitude of this vector and its expected value are related to the PMD value as:

$$\left\langle \vec{\Omega}_\omega \cdot \vec{\Omega}_\omega \right\rangle = \left\langle \left(\frac{d\Delta\tau}{d\omega} \right)^2 \right\rangle + \left\langle \Delta\tau^2 \frac{d\vec{p}}{d\omega} \cdot \frac{d\vec{p}}{d\omega} \right\rangle = \frac{1}{3} \left\langle \Delta\tau^2 \right\rangle^2 \quad (3-24)$$

The ratio of the first term, involving the derivative of the DGD, to the second term, involving the derivative of the PSP, is 1/8. The first term is interactive with chromatic dispersion and the second term has a depolarizing effect.

The convolution of the expanded representation of the frequency transfer matrix with the input pulse is beyond the scope of this clause, but it is clear that the results will not be as easy to represent and will depend on the details of the parameters at the frequency of the source. If, however, one is interested in the expected values, Equation 3-24 makes it clear that these values can be calculated from the PMD_{RMS} value and those explicit measurements are not needed.

3.1.7 PMD_Q : For a concatenated link comprised of M individual cable sections, the PMD link design value, PMD_Q , is defined as the value that the link PMD coefficient, X_M , exceeds with probability Q :

$$P(X_M > \text{PMD}_Q) = Q \quad (3-25)$$

PMD_Q is a parameter that represents a statistical extreme of the distribution of PMD values that result from a concatenation of M randomly selected sections with individual PMD coefficient values. The link PMD coefficient calculation is performed using the quadrature average formula. The statistical extreme is given at a confidence level defined as $1 - Q$, with Q being small. If $Q = 10^{-4}$, there is 99.99% confidence that the actual PMD coefficient of M concatenated cables will be less than or equal to PMD_Q .

3.2 Types of test methods

3.2.1 reference test method (RTM): A test method in which a characteristic of a specified class of optical fibres or optical fibre cables is measured strictly according to the definition of this characteristic and which gives results which are accurate, reproducible and relatable to practical use.

3.2.2 alternative test method (ATM): A test method in which a given characteristic of a specified class of optical fibres or optical fibre cables is measured in a manner consistent with the definition of this characteristic and which gives results which are reproducible and relatable to the reference test method and to practical use.

4 Abbreviations and acronyms

This Recommendation uses the following abbreviations and acronyms:

a.c.	alternating current
ASE	Amplified Spontaneous Emission
ATM	Alternative Test Method
DGD	Differential Group Delay
d.c.	direct current
DoP	Degree of Polarization
DSF	Dispersion-shifted Single-mode Fibre
EDFA	Erbium-Doped Fibre Amplifier
FCFT	Fast Cosine Fourier Transform

FFP	Far-Field Pattern
FFS	Far-Field Scan
FUT	Fibre Under Test
FWHM	Full Width at Half Maximum
GINTY	General analysis for the interferometric method
JME	Jones Matrix Eigenanalysis
LED	Light Emitting Diode
MFD	Mode Field Diameter
NFP	Near-Field Pattern
NFS	Near-Field Scan
OPGW	OPtical Ground Wire
PMD	Polarization Mode Dispersion
PMD_Q	Statistical parameter for link PMD
PMF	Polarization-Maintaining Fibre
PS	Poincaré Sphere
PSA	Poincaré Sphere Analysis
PSP	Principal State of Polarization
RMS	Root Mean Square
RTM	Reference Test Method
SBS	Stimulated Brillouin Scattering
SMF	Single-Mode Fibre
SNR	Signal-to-Noise Ratio
SOP	State Of Polarization
TINTY	Traditional analysis for the interferometric method
VA	Variable Aperture
VOA	Variable Optical Attenuator
WDM	Wavelength Division Multiplexing

5 Conventions

I/O-SOP State of polarization of an input polarizer setting and an orthogonal pair of analyser settings.

6 Test methods

Both reference test method (RTM) and alternative test methods (ATMs) are usually given here for each parameter and it is the intention that both the RTM and the ATM(s) may be suitable for normal product acceptance purposes. However, when using an ATM, should any discrepancy arise, it is recommended that the RTM be employed as the technique for providing the definitive measurement results.

NOTE – The apparatus and procedure given cover only the essential basic features of the test methods. It is assumed that the detailed instrumentation will incorporate all necessary measures to ensure stability, noise elimination, signal-to-noise ratio (SNR), etc.

6.1 Test methods for polarization mode dispersion

All the test methods report the PMD value. The conversion to PMD coefficient shall be done according to the definitions in clause 3.1.5. All procedures are restricted to wavelengths greater than or equal to that at which the fibre is effectively single mode.

6.1.1 Reference test method: The Stokes parameter evaluation technique

6.1.1.1 General

This test method describes a procedure for measuring the PMD of single-mode optical fibres. The change in the output state of polarization (SOP) with wavelength is determined. This change can be characterized through Jones matrix eigenanalysis (JME), or the rotation of the SOP vector on the Poincaré sphere (PS). It can be applied to both short and long fibres, regardless of the degree of polarization (DoP) mode coupling. Under some circumstances, repeated measurements may be necessary to achieve satisfactory precision.

When measuring fibres in motion [e.g., fibres in optical ground wire (OPGW)], the interferometer method could be a better choice for the dispute resolution function of the RTM.

6.1.1.2 Test apparatus

See Figure 1 for a schematic diagram of the key components of a typical measurement system.

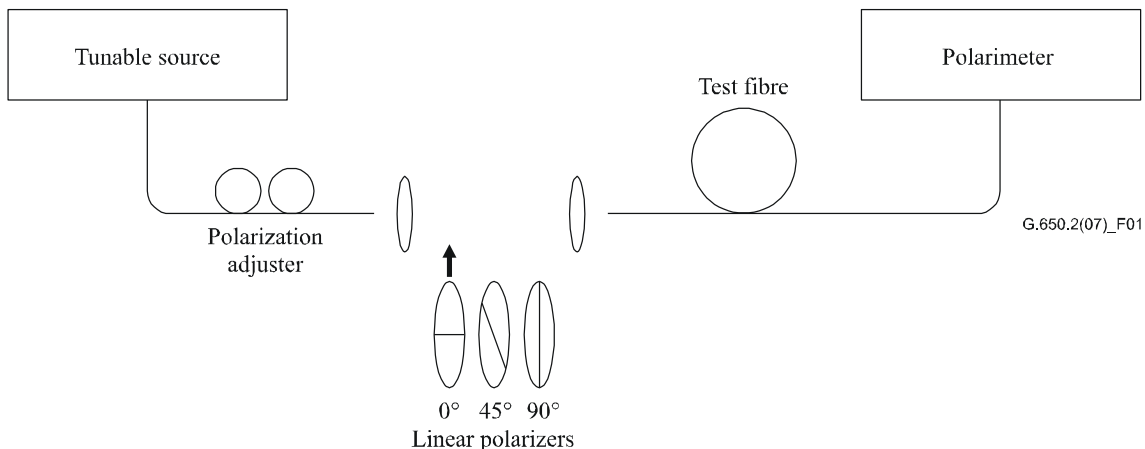


Figure 1 – Schematic diagram of equipment (typical)

6.1.1.2.1 Light source

Use a single-line laser or narrow-band source that is tunable across the intended measurement wavelength range. The spectral distribution shall be narrow enough so that the light emerging from the test fibre remains polarized under all conditions of the measurement. A DoP of 90% or greater is preferred, although measurements may be performed with values as low as 25% with reduced precision. For a given DGD, $\Delta\tau$, the lowest DoP which can result is given by:

$$DoP = 100 \exp \left[-\frac{1}{4 \ln 2} \left(\frac{\pi c \Delta\tau \Delta\lambda_{FWHM}}{\lambda_0^2} \right)^2 \right] \quad (6-1)$$

assuming a Gaussian spectrum of width $\Delta\lambda_{FWHM}$, where FWHM denotes full width at half maximum, centred at λ_0 . DoP is expressed as a percentage.

6.1.1.2.2 Polarization adjuster

A polarization adjuster follows the laser and is set to provide roughly circularly polarized light to the polarizers, so that the polarizers never cross polarization with their input light. Adjust polarization as follows. Set the tunable laser wavelength to the centre of the range to be measured. Insert each of the three polarizers into the beam and perform three corresponding power measurements at the output of the polarizers. Adjust the source polarization via the polarization adjuster such that the three powers fall within approximately a 3 dB range of one another. In an open beam version of the set-up, a waveplate may perform the polarization adjustment.

6.1.1.2.3 Polarizers

Three linear polarizers at relative angles of approximately 45° are arranged to be inserted into the light beam in turn. The actual relative angles shall be known.

6.1.1.2.4 Input optics

An optical lens system or single-mode fibre (SMF) pigtail may be employed to excite the test fibre.

6.1.1.2.5 Fibre pigtail

If pigtails are used, interference effects due to reflections should be avoided. This may require index-matching materials or angled cleaves. The pigtails shall be single mode.

6.1.1.2.6 Optical lens system

If an optical lens system is used, some suitable means, such as a vacuum chuck, shall be used to stably support the input end of the fibre.

6.1.1.2.7 Cladding mode stripper

Remove any cladding mode power from the test fibre. Under most circumstances, the fibre coating will perform this function; otherwise, employ a device that extracts cladding mode power.

6.1.1.2.8 Output optics

Couple all power emitted from the test fibre to the polarimeter. An optical lens system, a butt splice to an SMF pigtail or an index-matched coupling made directly to the detector system are examples of means that may be used.

6.1.1.2.9 Polarimeter

Use a polarimeter to measure the three output states of polarization corresponding to insertion of each of the three polarizers. The wavelength range of the polarimeter shall include the wavelengths produced by the light source.

6.1.1.3 Measurement procedure

The test sample shall be a known length of a single-mode optical fibre which may or may not be cabled. The sample and pigtails shall be fixed in position at a nominally constant temperature throughout the measurement. Temperature stability of the test device may be observed by viewing the output state of polarization of the test fibre on a PS display. In a time period corresponding to an adjacent pair of Jones matrix measurements, output polarization change should be small relative to the change produced by a wavelength increment.

NOTE – Although the test sample is normally a fibre, this test can also be performed on discrete components. In this case, PMD coefficient is not relevant.

It is important to minimize deployment-induced mode coupling when measuring uncabled fibres, which is done in order to support the primary requirements of cabled fibre PMD_Q . In this case, the fibre shall be supported in some manner (usually on a reel having a minimum wind radius of 150 mm), with essentially zero fibre tension (typically less than 5 g force), and no tensioned crossovers. These

deployment requirements can limit the length that can be measured, depending on the spool diameter, and can make the measurement a destructive one. Multi-layer windings are possible, but should be qualified by comparison with single-layer results on shorter lengths.

The measurement of uncabled fibre deployed on shipping spools is not recommended. PMD results with this deployment have been shown to be substantially less than what would be obtained in cable form for high PMD fibre and substantially greater than what would be obtained in cable form for low PMD fibre.

Couple the light source through the polarization adjuster to the polarizers.

Couple the output of the polarizers to the input of the fibre under test.

Couple the output of the fibre under test to the input of the polarimeter.

Select the wavelength interval, $\Delta\lambda$, over which the measurements are to be performed. The maximum allowable value of $\Delta\lambda$ (around λ_0) is set by the requirement:

$$\Delta\tau_{\max} \Delta\lambda \leq \frac{\lambda_0^2}{2c} \quad (6-2)$$

where $\Delta\tau_{\max}$ is the maximum expected DGD within the measurement wavelength range. For example, the product of maximum DGD and wavelength interval shall remain less than 4 ps nm at 1 550 nm and less than 2.8 ps nm at 1 300 nm. This requirement ensures that from one test wavelength to the next, the output state of polarization rotates less than 180° about the principal states axis of the PS. If a rough estimate of $\Delta\tau_{\max}$ cannot be made, perform a series of sample measurements across the wavelength range, each measurement using a closely spaced pair of wavelengths appropriate to the spectral width and minimum tuning step of the optical source. Multiply the maximum DGD measured in this way by a safety factor of three, substitute this value for $\Delta\tau_{\max}$ in Expression 6-2 and compute the value of $\Delta\lambda$ to be used in the actual measurement. If there is concern that the wavelength interval used for a measurement was too large, the measurement may be repeated with a smaller wavelength interval. If the shape of the curve of DGD vs wavelength and the mean DGD are essentially unchanged, the original wavelength interval was satisfactory.

Gather the measurement data. At the selected wavelengths, insert each of the polarizers and record corresponding Stokes parameters from the polarimeter.

6.1.1.4 Calculations or interpretation of result

There are two ways [JME and PS analysis (PSA)] of analysing the Stokes parameters that were measured in clause 6.1.1.3. Both analysis methods deduce the rotation of the output Stokes vectors at one optical frequency to the next frequency. The DGD is proportional to the rotation angle and inversely proportional to the frequency difference. The two methods are mathematically equivalent for first-order PMD for negligible PDL.

The Stokes parameters for a given wavelength are the normalized Stokes output vectors which are represented as \vec{H} , \vec{Q} and \vec{V} for relative input linear SOP angles of 0°, 45° and 90°, respectively.

In clause 6.1.3, wavelength is used to describe the measurement. Angular optical frequency, $\omega = 2\pi c/\lambda$ (THz), is the most useful metric for the calculations. The calculations below are given for a single pair of adjacent frequencies designated as ω_0 and $\omega_0 + \Delta\omega$. This pair yields a DGD value. The DGD values are calculated for each ascending pair of frequencies over a frequency range using the same calculations.

The average of all the DGD values is reported as the PMD value.

6.1.1.4.1 Jones matrix eigenanalysis

For a given frequency, use Equation 3-5 to convert the measured unit output Stokes vectors to Jones vectors by assuming that $0 \leq \theta \leq \pi$. The complex x and y elements of these vectors are designated as: h_x , h_y , q_x , q_y , v_x , and v_y . Using these, calculate the following ratios:

$$k_1 = h_x / h_y \quad k_2 = v_x / v_y \quad k_3 = q_x / q_y \quad k_4 = \frac{k_3 - k_2}{k_1 - k_3} \quad (6-3)$$

The assumption of $0 \leq \theta \leq \pi$ is not relevant because of the ratio calculations.

For the frequency, the Jones transfer matrix, T , is calculated as:

$$T = \begin{bmatrix} k_1 k_4 & k_2 \\ k_4 & 1 \end{bmatrix} \quad (6-4)$$

The actual transfer matrix is the matrix of Equation 6-4 times an unknown complex constant that is inversely proportional to the square root of the determinant of the calculated matrix. This constant is not needed for the rest of the calculations, however.

For a pair of frequencies, the Jones frequency transfer matrix, J , is calculated as:

$$J(\omega_0) = T(\omega_0 + \Delta\omega) T^{-1}(\omega_0) \quad (6-5)$$

Calculate the two eigenvalues, $\rho_1(\omega_0)$ and $\rho_2(\omega_0)$ of $J(\omega_0)$. The DGD, $\Delta\tau(\omega_0)$ is given as:

$$\Delta\tau(\omega_0) = \frac{|\arg(\rho_1(\omega_0)/\rho_2(\omega_0))|}{\Delta\omega} \quad (6-6)$$

where:

$$\arg(me^{i\theta}) = \theta \quad \text{with } m \text{ and } \theta \text{ both real, and } |\theta| < \pi.$$

The data may be displayed as a function of wavelength as shown in Figure 2 or as a histogram as in Figure 3.

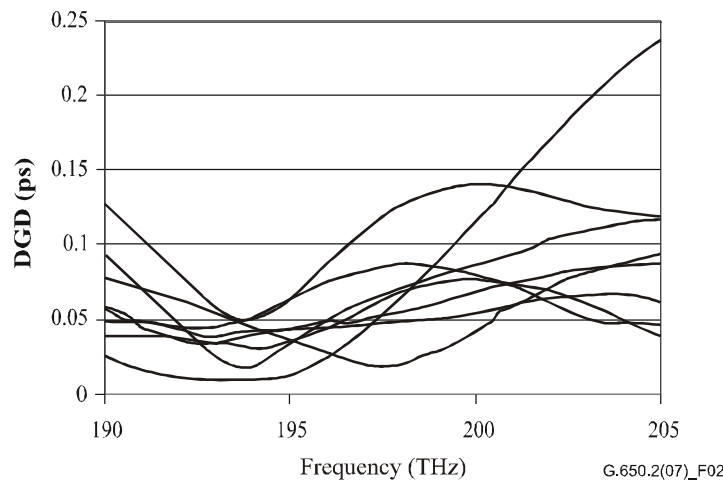


Figure 2 – DGD data vs frequency

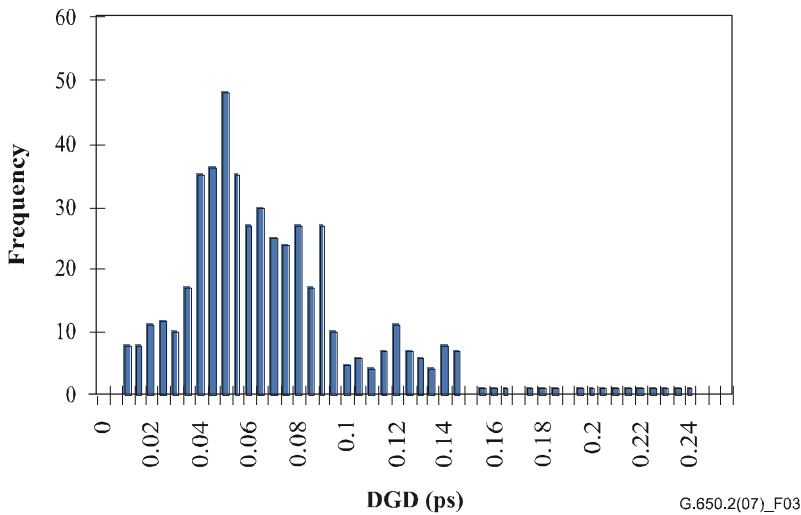


Figure 3 – DGD data as a histogram

6.1.1.4.2 Poincaré sphere analysis (PSA)

The analysis is based on an arcsine function to determine the rotation of the normalized Stokes vectors on the PS.

From the measured normalized Stokes vectors, \vec{H} , \vec{V} and \vec{Q} , compute:

$$\vec{h} = \vec{H}, \quad \vec{q} = \frac{\vec{H} \times \vec{Q}}{|\vec{H} \times \vec{Q}|} \times \vec{H}, \quad \vec{v} = \frac{\vec{q} \times \vec{V}}{|\vec{q} \times \vec{V}|} \times \vec{q} \quad (6-7)$$

This makes the analysis independent of the input SOPs, consequently there is no need to know their values.

From the Stokes vectors, \vec{h} , \vec{v} and \vec{q} , form the vector products $\vec{c} = \vec{h} \times \vec{q}$ and $\vec{c}' = \vec{q} \times \vec{v}$ at each wavelength. For each frequency increment, compute the finite differences,

$$\begin{aligned} \Delta\vec{h} &= \vec{h}(\omega_0 + \Delta\omega) - \vec{h}(\omega_0) & \Delta\vec{q} &= \vec{q}(\omega_0 + \Delta\omega) - \vec{q}(\omega_0) & \Delta\vec{v} &= \vec{v}(\omega_0 + \Delta\omega) - \vec{v}(\omega_0) \\ \Delta\vec{c} &= \vec{c}(\omega_0 + \Delta\omega) - \vec{c}(\omega_0) & \Delta\vec{c}' &= \vec{c}'(\omega_0 + \Delta\omega) - \vec{c}'(\omega_0) \end{aligned} \quad (6-8)$$

Find the DGD, $\Delta\tau$, for a particular frequency increment from Equation 6-9:

$$\Delta\tau = \frac{1}{\Delta\omega} \cdot \left[\arcsin\left(\frac{1}{2} \sqrt{\frac{1}{2} (\Delta\vec{h}^2 + \Delta\vec{q}^2 + \Delta\vec{c}^2)}\right) + \arcsin\left(\frac{1}{2} \sqrt{\frac{1}{2} (\Delta\vec{q}^2 + \Delta\vec{v}^2 + \Delta\vec{c}'^2)}\right) \right] \quad (6-9)$$

NOTE – $\Delta\vec{h}^2 = \Delta\vec{h} \cdot \Delta\vec{h}$.

6.1.1.5 Presentation of the results

The following details shall be presented:

- a) Identification of the sample measured.
- b) Test length.
- c) The wavelength range over which the measurement was performed, the wavelength step size, and the number of sampled points.
- d) The physical configuration of the fibre or cable sample.
- e) Mode-coupling type (negligible, semi-random or random).
- f) Method of analysis (JME or PS).

- g) PMD in picoseconds. If the degree of mode coupling is known, the PMD coefficient may be given in picoseconds per kilometre (negligible mode coupling) or picoseconds per root kilometre (random mode coupling).
- h) When an average PMD has been determined from repeated measurements of the sample, record the number of measurements performed.

6.1.2 First alternative test method: State of polarization (SOP) method

This method has been shown to be incomplete and has therefore been removed. Consequently, the method is only fundamentally valid in negligible mode coupling, but it is not valid in random mode coupling. For more information pertaining to PMD theory, see [b-IEC/TR 61282-9].

6.1.3 Second alternative test method: Interferometric method

6.1.3.1 General

This test method describes a procedure for measuring the PMD of single-mode optical fibres and cables.

The measured value represents PMD_{RMS} over a broad measurement wavelength range of typical broadband sources, such as a light-emitting diode (LED), combination of super LEDs or amplified spontaneous emission (ASE) source in the 1 310 nm or the 1 550 nm window or any other window of interest, depending on user requirements.

The PMD is determined from an interferogram containing the autocorrelation and cross-correlation function of the emerging electromagnetic field at one end of the fibre under test (FUT) when illuminated by the broadband polarized source at the other end.

The main advantage of this method is that the measurement time is very fast and the equipment can be easily used in the field. The dynamics and stability are provided by the well-established Fourier transform spectroscopy technique.

The fibre shall be single mode in the measured wavelength range.

The INTY method uses two analyses that entail slightly different measurements:

- Traditional analysis for the interferometric method (TINTY) using a set of specific operating conditions for its successful applications and a basic set-up.
- General analysis for the interferometric method (GINTY) using no limiting operating conditions, but using a modified set-up compared to TINTY.

6.1.3.2 Test apparatus

A generic set-up is shown in Figure 4, which is the basis of INTY experimental implementation. Variations of this set-up are possible and are shown below. The interferometer can be an air path type or a fibre type, it can be of the Michelson or Mach-Zehnder type and it can be located at the source or at the detector end. Examples are given in Figures 5, 6 and 7.

NOTE – When a fibre-type interferometer is used, care should be given to the fibre chromatic dispersion that may add to the measurement uncertainties.

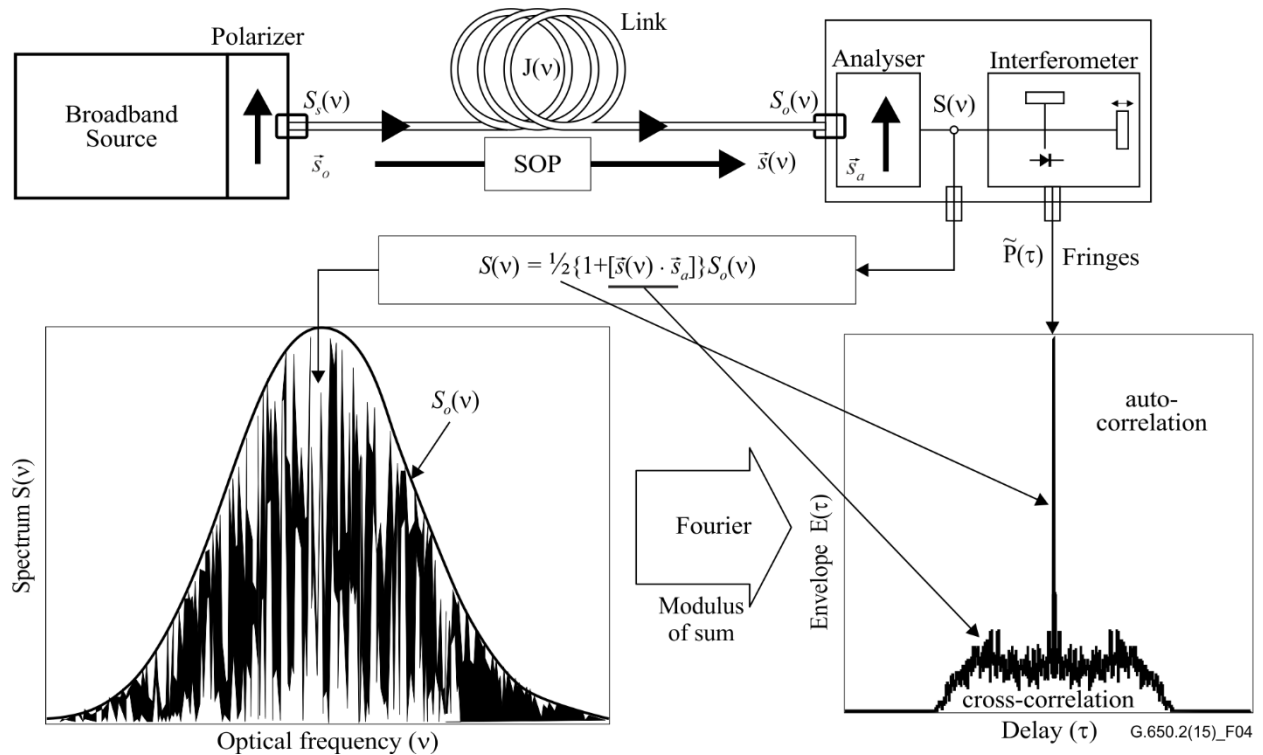


Figure 4 – Generic set-up for the interferometric technique

Parameters used in Figure 4 and throughout this Recommendation:

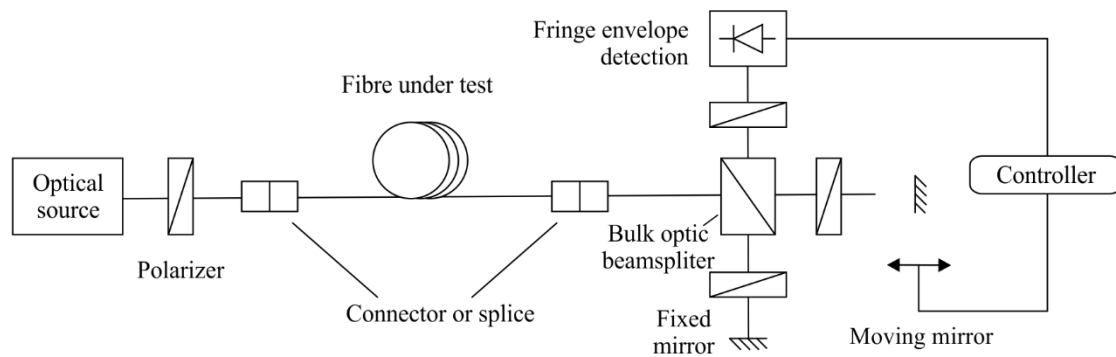
- v optical frequency ($\lambda v = c$)
- τ difference of round-trip delay between the two arms of the interferometer
- $S_s(v)$ optical spectrum, at FUT input \equiv spectral density of $\vec{E}_s(v)$ the source electric field spectrum
- $S_o(v)$ optical spectrum, at FUT output (analyser input)
- $S(v)$ optical spectrum, at analyser output (interferometer input)
- \vec{s}_0 input SOP (at FUT input; a unit Stokes vector)
- $\vec{s}(v)$ output SOP (at FUT output)
- \vec{s}_a analyser transmission axis
- $\vec{s}(v) \cdot \vec{s}_a$ Stokes parameter giving the projection of $\vec{s}(v)$ on the analyser transmission axis.
It is this parameter that contains the PMD information
- $P(\tau)$ optical power at the interferometer output, as a function of delay τ
- $\tilde{P}(\tau)$ τ -dependent part of $P(\tau)$ [alternating current (a.c.) part]
- P_0 constant part of $P(\tau)$ [direct current (d.c.) parts]
- $E(\tau)$ fringe envelope
- $E_x(\tau)$ cross-correlation envelope
- $E_0(\tau)$ autocorrelation envelope

The optical power at the interferometer output, $P(\tau)$, is equal to the sum of a.c. and d.c. parts. Both parts are equal at $\tau = 0$ so the a.c. part can be calculated. For an ideal interferometer, the a.c. part is an even function, the right half of which is equal to the cosine Fourier transform of the optical

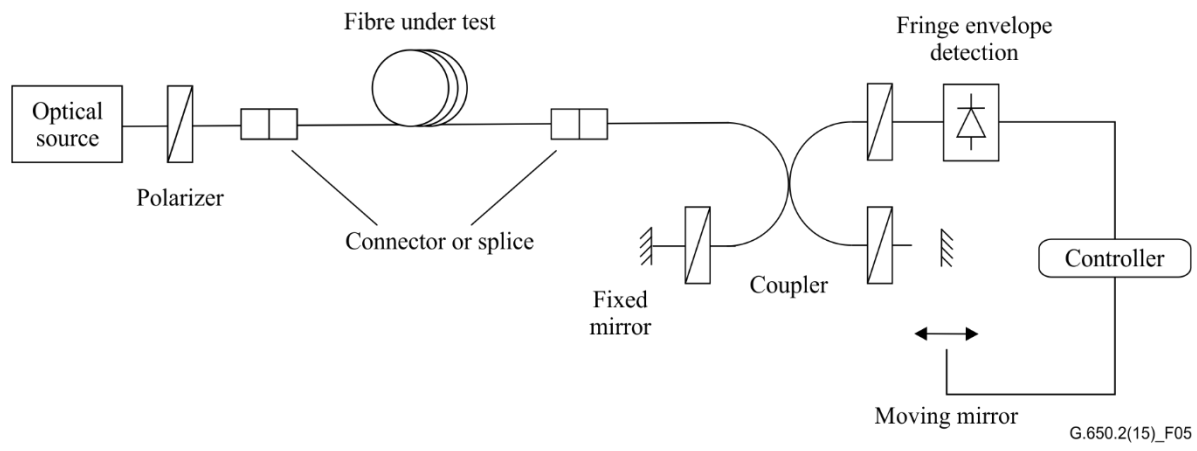
spectrum, $S(\nu)$, emitted from the analyser. For non-ideal interferometers, some corrections may be applied, depending on the details of the implementation.

For TINTY, the envelope of the interferogram, $E(\tau)$, is the absolute value of the a.c. part. For GINTY, additional calculations to obtain the cross-correlation and autocorrelation envelopes are described in clause 6.1.3.4.2. These calculations involve two measured interferograms resulting from the analyser being set at two orthogonal SOPs.

Other set-ups are shown in Figures 5, 6 and 7.



a) With bulk optic beam splitter



b) With fibre coupler

Figure 5 – The interferometric method using a Michelson interferometer

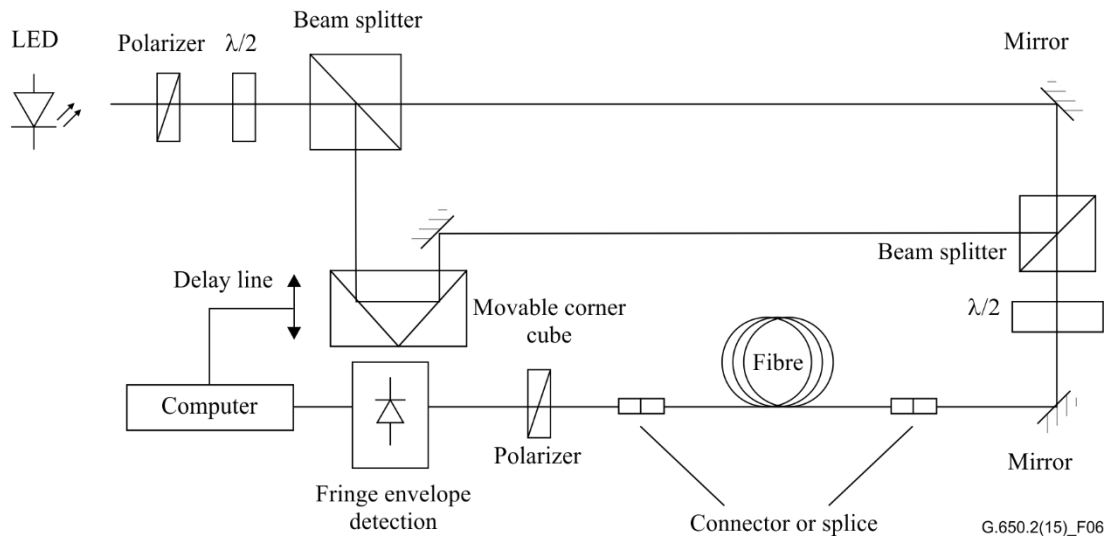


Figure 6 – The interferometric method using a Mach–Zehnder type interferometer with an air path

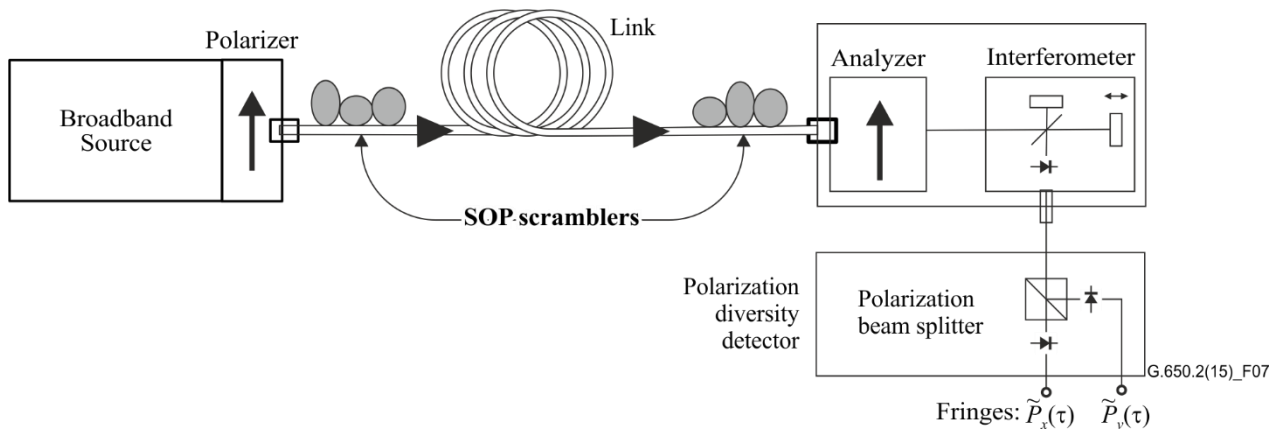


Figure 7 – The GINTY using I/O-SOP scrambling and a polarization diversity detector

6.1.3.2.1 Optical source

A polarized broad spectrum source, such as an LED, set of super LEDs or ASE source followed by a polarizer, shall be used. The centre wavelength of the light source shall be within the O-band or the C-band, or within any band of interest. A typical value of the source linewidth is about 60 nm or larger FWHM. TINTY requires that the spectral shape of the source shall be approximately Gaussian, without ripples which could influence the autocorrelation function of the emerging light. GINTY does not impose any such requirements. The source linewidth (also called spectral width in the LED field), $\Delta\lambda$, must be known to calculate the coherence time, t_c , which is determined using Equation 6-10:

$$t_c = \frac{\lambda_0^2}{\Delta\lambda c} \quad (6-10)$$

where:

λ_0 is the source centre wavelength

$\Delta\lambda$ is the source linewidth

c is the speed of light in a vacuum

6.1.3.2.2 Analyser

The analyser shall polarize the light over the full wavelength range of the source. For GINTY, the analyser must be capable of being rotated to a setting orthogonal to the initial setting.

6.1.3.2.3 Polarization scramblers (optional)

In Figure 7, the polarization scrambler allows the selection of any SOPs for the FUT input and output. The polarization beamsplitter allows simultaneous detection of what would be detected by two orthogonal analyser settings. The functionality of the polarization scrambler selecting various SOPs for the input and various analyser settings at the output can be achieved by other means.

6.1.3.2.4 Interferometer beamsplitter

The beamsplitter of the interferometer is used to split the incident polarized light into two components propagating in the interferometer's arms. The beamsplitter can be a fibre coupler as shown in Figure 5-b or a bulk optic beamsplitter as shown in Figure 5-a.

6.1.3.2.5 Detector

The light emerging from the FUT is coupled to a photodetector whose SNR is adequate for the measurement. The detection system may include synchronous detection by chopper and lock-in amplifier or comparable techniques.

6.1.3.2.6 Computer

For the analysis of the interference pattern, a computer with suitable software shall be used.

6.1.3.3 Samples

The FUT sample shall be of known length of SMF that may or may not be cabled. The sample and pigtails must be fixed in position at a nominally constant temperature throughout the measurement. The standard ambient conditions shall be employed. In the case of installed fibres and cables, prevailing deployment conditions may be used.

It is important to minimize deployment-induced mode coupling when measuring uncabled fibres, which is done in order to support the primary requirements of cabled fibre PMD_Q . In this case, the fibre shall be supported in some manner (usually on a reel having a minimum wind radius of 150 mm), with essentially zero fibre tension (typically less than 0.05 N or 5 g force), and no tensioned crossovers. These deployment requirements can limit the length that can be measured, depending on the spool diameter, and can make the measurement a destructive one. Multi-layer windings are possible, but should be qualified by comparison with single-layer results on shorter lengths.

The measurement of uncabled fibre deployed on shipping spools is not recommended. PMD results with this deployment have been shown to be substantially less than those obtained in cable form for high PMD fibre and substantially greater than those obtained in cable form for low PMD fibre.

NOTE – Although the test sample is normally a fibre, this test can also be performed on discrete components. In this case, PMD coefficient is not relevant. However, in the case of TINTY, PMD resolution is always limited by the width of the autocorrelation peak (typically in the 100 fs range). GINTY does not suffer from such limitations and PMD resolutions limited solely by the instrument implementation uncertainties can be achieved (typically in the 10 fs range or less).

6.1.3.4 Procedure

One end of the FUT is coupled to the polarized output of the polarized light source. The other end is coupled to the output optics. This can be done by standard fibre connectors, splices or by a fibre alignment system. If the latter is used, some index-matching oil should be used to avoid reflections.

The optical output power of the light source is adjusted to a reference value characteristic for the detection system used. To get a sufficient fringe contrast, the optical power in both arms shall be almost identical.

6.1.3.4.1 TINTY procedure

Make a first acquisition in moving the mirror of the interferometer arm and recording the intensity of the light. Subtract the value found for $\tau = 0$ from the interferogram to obtain $\tilde{P}(\tau)$. The absolute value of $\tilde{P}(\tau)$ is the fringe envelope, $E(\tau)$.

From the fringe pattern obtained for one selected state of polarization, the PMD delay can be calculated as described below. A typical example of a fringe pattern for low and high polarization mode coupling is shown in Figure 8.

If mode coupling is insufficient or the PMD is low, it is recommended that the measurement be repeated for different SOPs or the SOP modulated during the measurement in order to obtain a result which is an average over all SOPs.

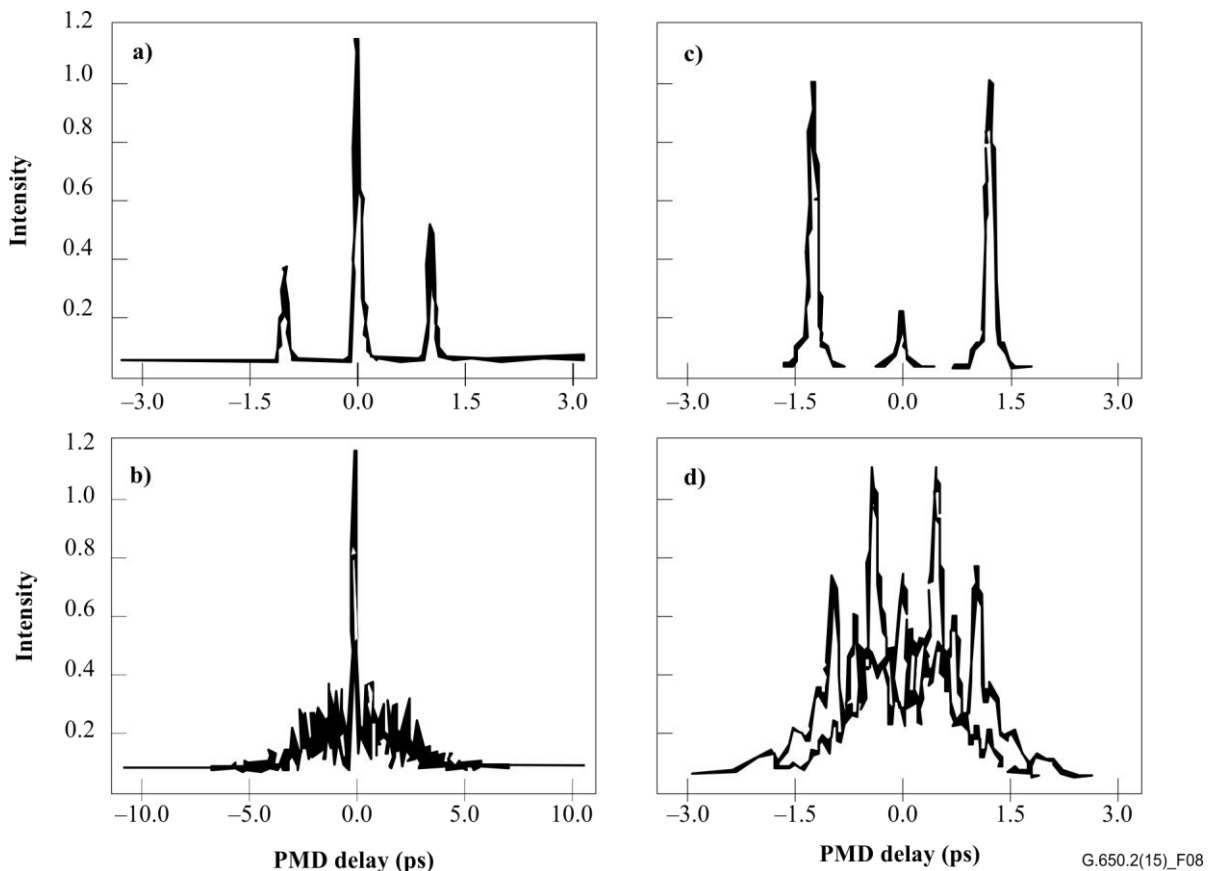


Figure 8 – Example of a fringe pattern obtained with the autocorrelation type instrument (a, b) and with the cross-correlation type instrument (c, d) for negligible (top) and random (bottom) polarization mode coupling

The fringe envelopes obtained from TINTY are a combination of the cross-correlation and autocorrelation functions. An algorithm must be used to try to separate out the part that is from the cross-correlation function.

6.1.3.4.2 GINTY procedure

The combination of a particular input polarizer setting and an orthogonal pair of analyser settings is called an I/O-SOP. Complete the scan(s) for the two interferograms and subtract the d.c. part from each to obtain $\tilde{P}_x(\tau)$ and $\tilde{P}_y(\tau)$, the orthogonally generated fringes.

The cross-correlation and autocorrelation fringe envelopes, $E_x(\tau)$ and $E_0(\tau)$ are calculated as:

$$E_x(\tau) = |\tilde{P}_x(\tau) - \tilde{P}_y(\tau)| \quad E_0(\tau) = |\tilde{P}_x(\tau) + \tilde{P}_y(\tau)| \quad (6-11)$$

These functions are squared for the purposes of later calculations and display. Some examples of squared cross-correlation results are shown in Figures 9, 10 and 11. Note that the autocorrelation peak seen with the TINTY is not present.

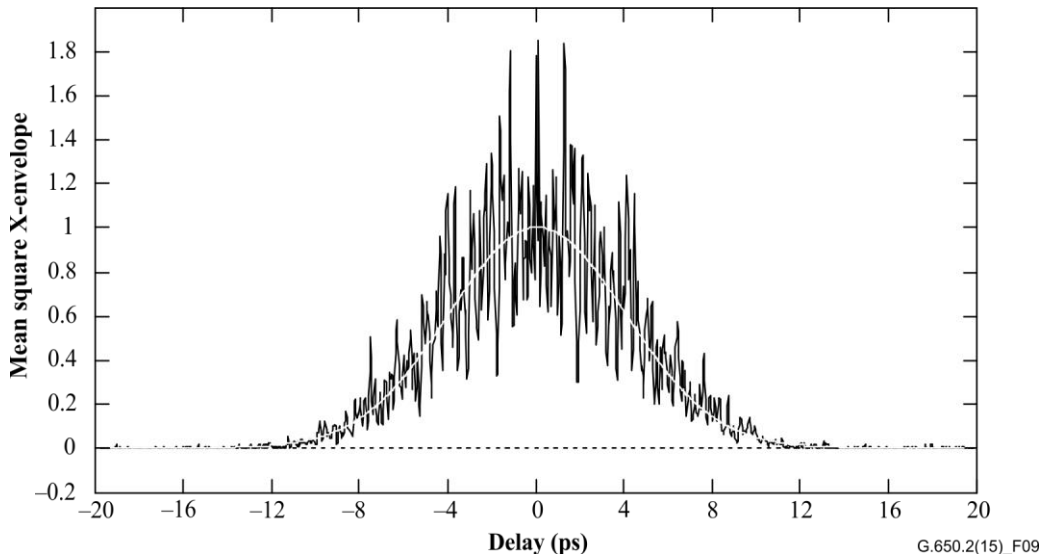


Figure 9 – Example of a fringe pattern obtained with GINTY and I/O-SOP scrambling for random mode coupling

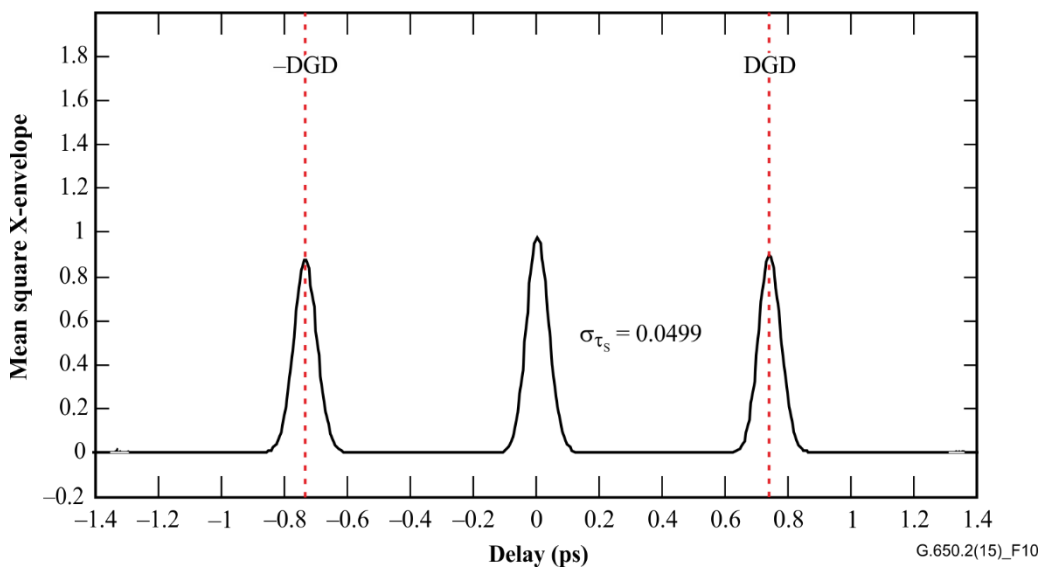


Figure 10 – Example of a fringe pattern obtained with GINTY and I/O-SOP scrambling for negligible mode coupling

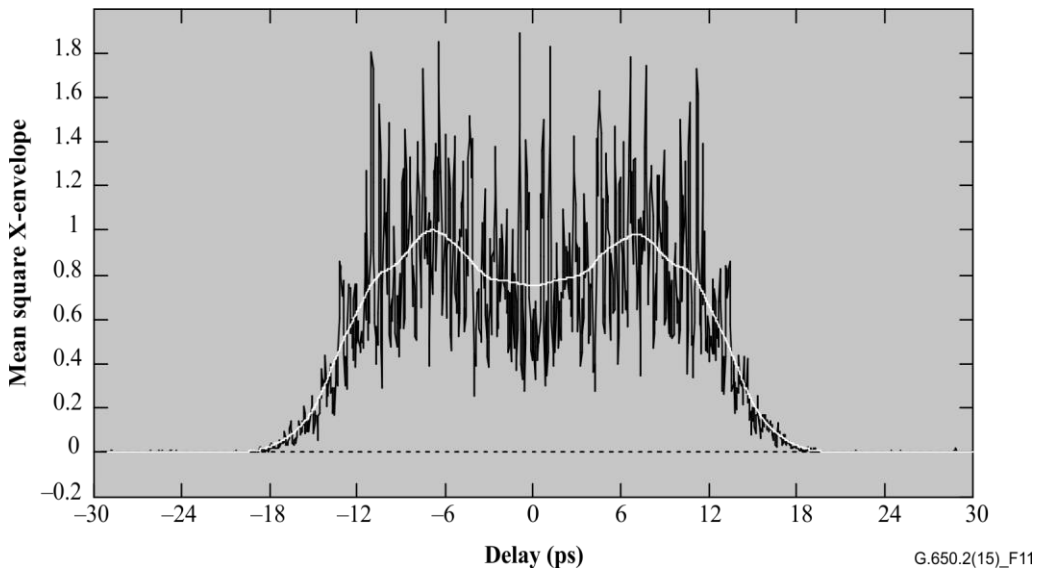


Figure 11 – Example of a fringe pattern obtained with GINTY and I/O-SOP scrambling for mixed mode coupling

Options for polarization scrambling follow. When multiple I/O-SOPs are measured, distinguish them by adding a subscript i , where $i = 1, 2, 3 \dots$, for later calculations.

6.1.3.4.2.1 The nine state Mueller set

The sum of nine squared envelopes observed with nine specific I/O-SOPs is rigorously equal to the uniformly scrambled mean squared envelope. These nine I/O-SOPs are: three analyser-axes forming a right-angled trihedron, for each three input SOPs also forming a right-angled trihedron.

6.1.3.4.2.2 Random scrambling

Scan-to-scan scrambling: Automatic/manual setting of the scramblers at each scan.

Continuous scrambling: When squared envelopes are summed, scrambling can be performed while scanning. Automated scramblers are set to cover the sphere continuously as a function of time.

Fast, single-scan scrambling: If scramblers are sufficiently fast, well-scrambled squared envelopes can be observed in a single-scan. However, this requires special provisions to avoid crosstalk between the a.c. part and the previously d.c. part of the interferogram.

6.1.3.5 Calculations

Both these calculations report PMD_{RMS}. For ideal random mode coupling when the interferogram is of an ideal Gaussian shape, this may be converted to PMD_{Avg} using Equation 3-3.

6.1.3.5.1 TINTY calculations

For negligible mode coupling, the separation of the single well-defined peaks from the centre is the DGD value, which is also the PMD value.

The following calculations are suitable for the random mode-coupling regime associated with long fibres/cables or links. The spread in the fringe envelope, discounting the centre peak, is characterized.

The PMD_{RMS} value is determined from the second moment (RMS width) of the cross-correlation function of the detected signal (fringe envelope).

$$\text{PMD}_{\text{RMS}} = \left(\sqrt{\frac{3}{4}} \right) \sigma_{\varepsilon} \quad (6-12)$$

where:

σ_ε is the RMS width of the cross-correlation envelope

A detailed algorithm for the calculation of σ_ε from a measured fringe envelope is described in clause I.1.

For certain assumptions given below, Equation 6-12 can be related to Equation 3-2 as:

$$\langle \Delta\tau^2 \rangle = \frac{3}{4} \langle \sigma_\varepsilon^2 \rangle \quad (6-13)$$

Equation 6-13 is obtained from the theory given the following assumptions:

- Ideal random mode coupling.

NOTE 1 – Ideal random coupling means $L/h \rightarrow \infty$, and a uniformly distributed birefringence axis. L is the device length and h is the polarization coupling-length. For a device consisting of N concatenated birefringent segments of length h , this corresponds to $N \rightarrow \infty$ with uniformly distributed axes.

NOTE 2 – Analysis of no (or negligible) mode coupling is possible.

- A purely Gaussian source, with no ripples.
- $\text{PMD} \gg \sigma_0$

where:

σ_0 is the RMS width of the auto-correlation envelope;

- Ergodic conditions.

NOTE 3 – Given that the source is Gaussian, the result must be some form of weighted average of the DGD values. This weighting is not specified in TINTY, but is in GINTY. For this reason, this method is expected to give a different result for a given wavelength range and time than one of the methods that use a rectangular weighting (e.g., the RTM). The assumption of ergodic conditions does result in the validity of the expected value relationship. In practice, the wavelength ranges sampled by different implementations of the other methods will also vary, which would also imply getting different results from each implementation.

6.1.3.5.2 GINTY calculations

GINTY allows some of the assumptions required for Equation 6-13 with TINTY to be removed. Notably:

- the assumption of ideal random mode coupling is not required;
- the assumption of a Gaussian source is not required;
- the assumption that the PMD is large compared to the width of the autocorrelation function is not required.

Form the mean squared cross-correlation and autocorrelation envelopes, $\bar{E}_x^2(\tau)$ and $\bar{E}_0^2(\tau)$ as:

$$\bar{E}_x^2(\tau) = \frac{1}{N} \sum_i E_{xi}^2(\tau) \quad \bar{E}_0^2(\tau) = \frac{1}{N} \sum_i E_{0i}^2(\tau) \quad (6-14)$$

where N is the number of I/O-SOPs.

Calculate the RMS width of the two sampled mean squared envelopes, σ_0 and σ_x , respectively. A sample algorithm for this calculation is given in clause I.2. The mathematical definitions of these widths are:

$$\sigma_x^2 = \frac{\int \tau^2(\tau) \langle E_x^2(\tau) \rangle d\tau}{\int \langle E_x^2(\tau) \rangle d\tau} \quad \sigma_0^2 = \frac{\int \tau^2(\tau) \langle E_0^2(\tau) \rangle d\tau}{\int \langle E_0^2(\tau) \rangle d\tau} \quad (6-15)$$

The expected value operator in the above equations is with respect to a uniform and random sampling of the I/O-SOPs.

The PMD_{RMS} value that is reported is:

$$\text{PMD}_{\text{RMS}} = \left[\frac{3}{2} (\sigma_x^2 - \sigma_0^2) \right]^{1/2} \quad (6-16)$$

Equation 6-16 relates to Equation 3-2 as:

$$\frac{\int \Delta\tau^2(v) S_0^2(v) dv}{\int S_0^2(v) dv} = \frac{3}{2} (\sigma_x^2 - \sigma_0^2) \quad (6-17)$$

Using the ideal definitions of the RMS width terms from Equation 6-15, Equation 6-17 is exact for any DGD curve present at the time of measurement and any source spectral characteristics. The left side of Equation 6-17 is a spectrally weighted (by squared power) RMS calculation.

Using the assumption of ergodic conditions:

$$\langle \Delta\tau^2 \rangle = \left\langle \frac{\int \Delta\tau^2(v) S_0^2(v) dv}{\int S_0^2(v) dv} \right\rangle \quad (6-18)$$

6.1.3.6 Presentation of the results

The following details shall be presented:

- a) Date.
- b) Fibre identification.
- c) Fibre type.
- d) Fibre length.
- e) Test set-up arrangement, including source type, wavelength, linewidth (FWHM).
- f) Launching technique.
- g) Type of fringe detection technique.
- h) Plot over the scanned range with fringe pattern (only if mode-coupling type is not random).
- i) Fibre deployment and environmental conditions (radius, stress, temperature, etc.).
- j) Mode-coupling type (random, mixed or negligible).
- k) Analysis method (TINTY or GINTY)
- l) PMD_{RMS} , in picoseconds, or PMD_{AVG} (specify which), in picoseconds, and PMD coefficient. If the degree of mode coupling is known, the coefficient may be given in picoseconds per kilometre or picoseconds per root kilometre.

6.1.4 Third alternative test method: Fixed analyser technique

6.1.4.1 General

This test method describes a procedure for measuring the PMD of single-mode optical fibres. It produces a single measurement value that represents the PMD over the measurement wavelength range of typically a few hundred nanometres. The method can be applied to both short and long fibres in the limits of both negligible and random polarization mode coupling. Under some circumstances, repeated measurements may be necessary to achieve satisfactory precision using this method. The procedure is restricted to wavelengths greater than or equal to that at which the fibre is effectively single mode.

6.1.4.2 Test apparatus

See Figure 12 for a schematic diagram of the key components in a typical measurement system.

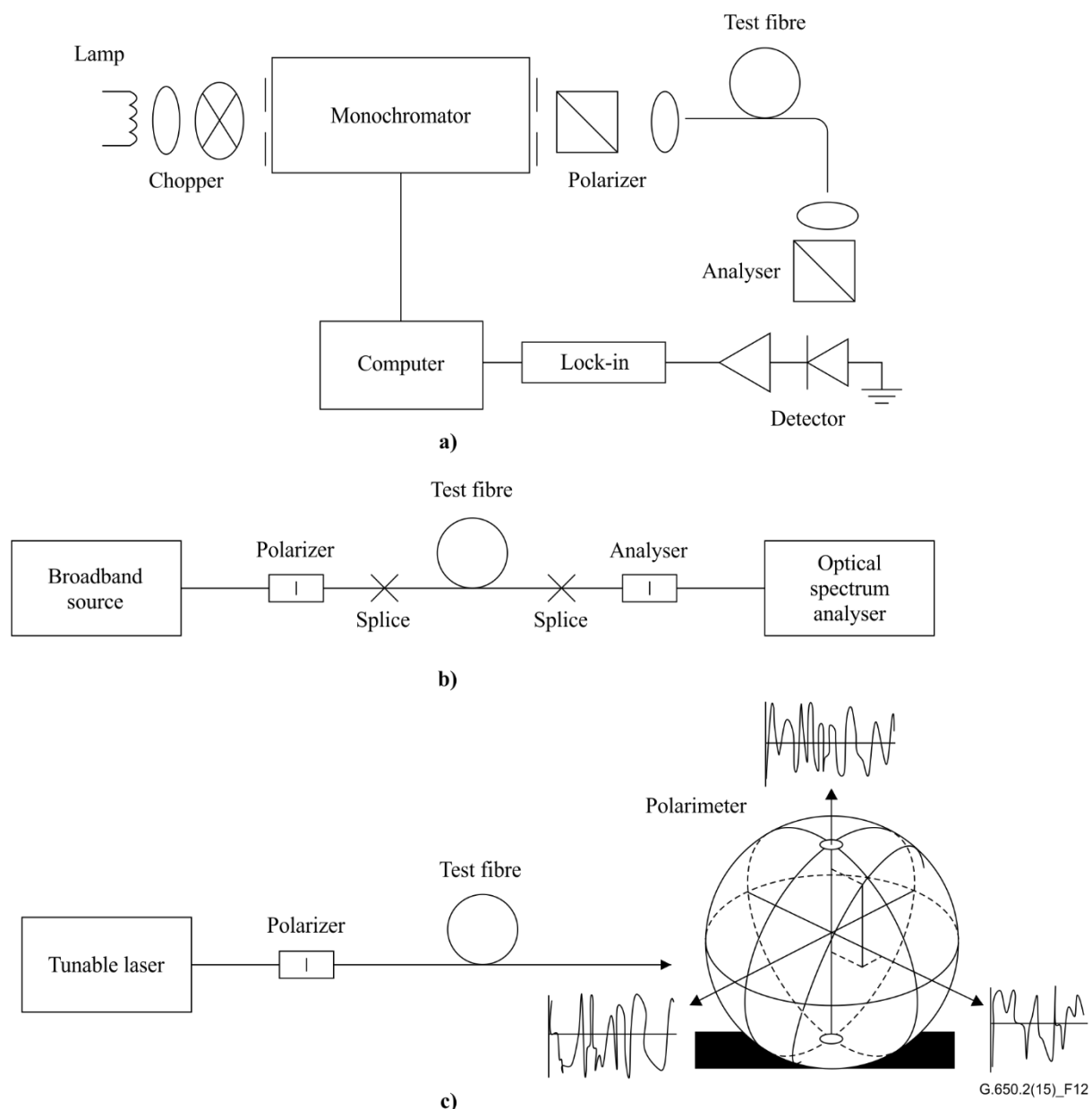


Figure 12 – Schematic diagram of equipment (typical)

6.1.4.2.1 Light source

Use a light source which emits radiation at the intended measurement wavelengths, such as a broadband lamp, light emitting diode(s) or tunable laser(s). It shall be stable in intensity and spectral distribution over a time period long enough to perform the measurement.

6.1.4.2.2 Monochromator

Obtain a specified set of test wavelengths by filtering the light source with a monochromator as in Figure 12-a, or by using an optical spectrum analyser as the detector, as in Figure 12-b. This filtering is not needed when the source is a tunable laser (see Figure 12-c). The spectral distribution must be narrow enough to avoid major depolarization of the signal under the influence of the PMD of the fibre under test (see clauses 6.1.4.4.1.4 and 6.1.4.4.2.8).

6.1.4.2.3 Input optics

An optical lens system or SMF pigtail may be employed to excite the test fibre. The power coupled into the fibre shall be stable for the duration of the test. If pigtailed are used, interference effects due to reflections should be avoided. This may require index-matching materials or angled cleaves. The pigtailed shall be single mode.

If an optical lens system is used, some suitable means, such as a vacuum chuck, shall be used to stably support the input end of the fibre.

6.1.4.2.4 Cladding mode stripper

Remove any cladding mode power from the test fibre. Under most circumstances, the fibre coating performs this function; otherwise, employ a device that extracts cladding mode power.

6.1.4.2.5 Output optics

All power emitted from the test fibre must be coupled onto the active region of the detection system (see Figure 12). An optical lens system, a butt splice to an SMF pigtail or an index-matched fibre-to-fibre coupling made directly to the detection system are examples of means that may be used.

6.1.4.2.6 Signal detection

For signal detection, use an optical detector that is linear and stable over the range of intensities and measurement times that are encountered in performing the measurement. A typical system might include synchronous detection by a chopper and lock-in amplifier, an optical power meter, an optical spectrum analyser or a polarimeter. To use the entire spectral range of the source, the detection system must have a wavelength range which includes the wavelengths produced by the light source.

6.1.4.2.7 Polarizer and analyser

The polarizer at the fibre input (Figure 12) is needed only if the launch beam is not already polarized (usually a 3 dB extinction ratio is sufficient). The angular orientation of the polarizers is not critical, but should remain fixed throughout the measurement. With negligible mode coupling, some adjustment of the polarizer orientation may be helpful in maximizing the amplitude of the oscillations in Figure 13-a. Alternatively, this may be achieved by rotation of the fibre(s) at splices or connectors.

The analyser is not needed when a polarimeter is used for signal detection (Figure 12-c).

6.1.4.3 Measurement procedure

The test sample shall be a known length of a single-mode optical fibre that may or may not be cabled. The sample and pigtailed must be fixed in position at a nominally constant temperature throughout the measurement.

NOTE – Although the test sample is normally a fibre, this test can also be performed on discrete components. In this case, PMD coefficient is not relevant.

Temperature stability of the test device may be observed by measuring the output power from the fibre at a fixed wavelength, with the output analyser in place. In a time period corresponding to a typical complete measurement, the output power change should be small relative to the changes produced by a wavelength increment.

It is important to minimize deployment-induced mode coupling when measuring uncabled fibres, which is done in order to support the primary requirements of cabled fibre PMD ϱ . In this case, the fibre shall be supported in some manner (usually on a reel having a minimum wind radius of 150 mm), with essentially zero fibre tension (typically less than 5 g force), and no tensioned crossovers. These deployment requirements can limit the length that can be measured, depending on the spool diameter, and can make the measurement a destructive one. Multi-layer windings are possible, but should be qualified by comparison with single-layer results on shorter lengths.

The measurement of uncabled fibre deployed on shipping spools is not recommended. PMD results with this deployment have been shown to be substantially less than what would be obtained in cable form for high PMD fibre and substantially greater than what would be obtained in cable form for low PMD fibre.

Couple the input end of the fibre to the light source. Couple the output radiation from the fibre under test to the detection system.

By making appropriate adjustments to the monochromator, optical spectrum analyser or tunable laser, inject each designated test wavelength λ in turn into the fibre. The choice of wavelengths depends on the designated wavelength scan range and also on the analysis method (see clauses 6.1.4.4.1 and 6.1.4.4.2).

Record the corresponding output signal for each wavelength. This process shall be accomplished without changing the launch and detector conditions. Call the received power $P_A(\lambda)$, where A denotes the presence of the analyser.

Remove the analyser from the beam and repeat the monochromator scan. Call this received power $P_{TOT}(\lambda)$. This latter power can be used to eliminate the spectral dependence of the measurement system components and the test fibre loss. Typical plots of the ratio:

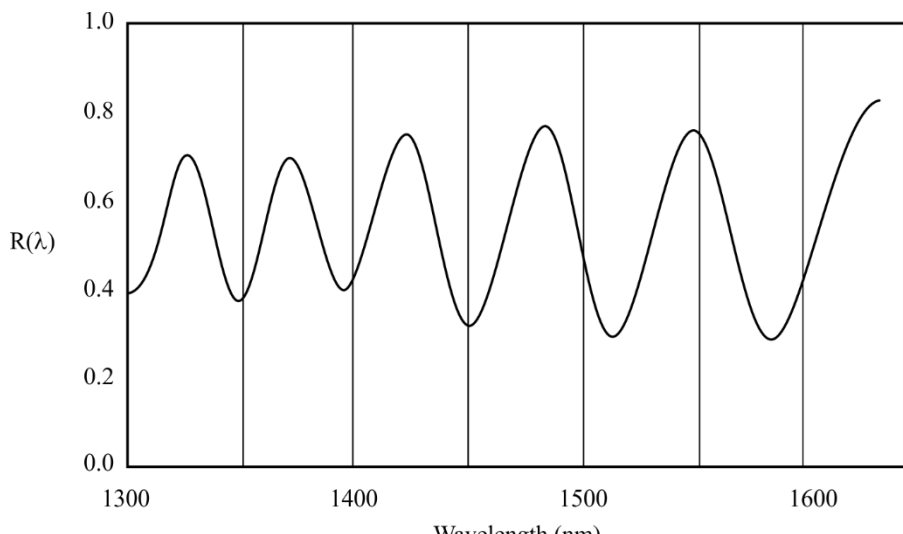
$$R(\lambda) = \frac{P_A(\lambda)}{P_{TOT}(\lambda)} \quad (6-19)$$

are shown in Figure 13.

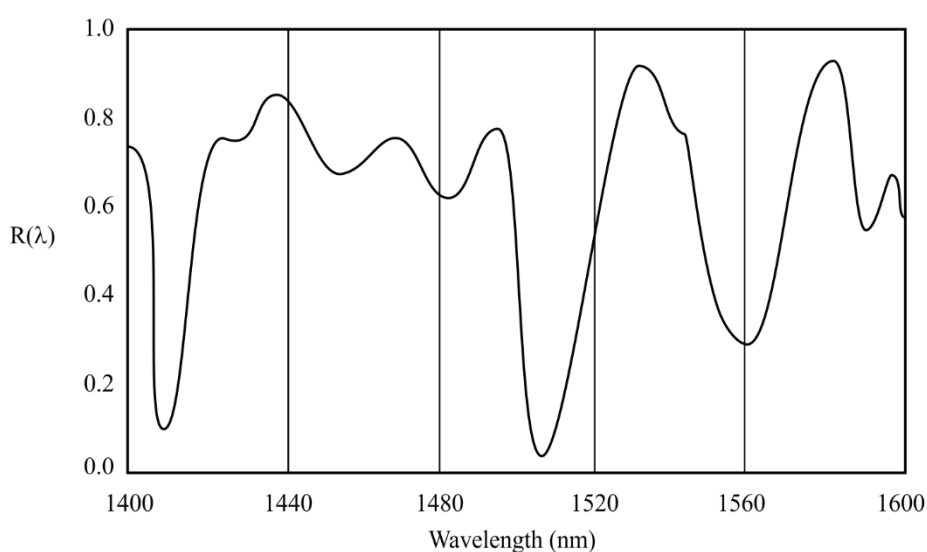
An alternative procedure is to leave the analyser in place, but rotate it 90° with respect to the orientation used above. Calling the power received in this case $P_{ROT}(\lambda)$, then:

$$R(\lambda) = \frac{P_A(\lambda)}{P_A(\lambda) + P_{ROT}(\lambda)} \quad (6-20)$$

If a polarimeter is used as the detection element, the normalized Stokes parameters are measured versus wavelength. The three spectral functions are independent of the received power and are analysed by the same methods applied to $R(\lambda)$ (see clauses 6.1.4.4.1 and 6.1.4.4.2). Each normalized Stokes parameter then leads to a value of $\langle \Delta\tau \rangle$.



a) Negligible mode coupling



b) Random mode coupling

G.650.2(15)_F13

Figure 13 – Typical data obtained in measuring PMD

6.1.4.4 Calculations or interpretation of results

One of the following two methods (clauses 6.1.4.4.1 and 6.1.4.4.2) shall be used for calculating PMD from the measurement data.

6.1.4.4.1 Extrema counting

6.1.4.4.1.1 PMD

$R(\lambda)$ should be obtained at evenly spaced wavelength intervals. E is the number of extrema within the window $\lambda_1 < \lambda < \lambda_2$. Alternatively, λ_1 and λ_2 may be chosen to coincide with extrema, in which case E is the number of extrema (including the ones at λ_1 and λ_2) minus one.

$$\langle \Delta\tau \rangle = \frac{k E \lambda_1 \lambda_2}{2(\lambda_2 - \lambda_1)c} \quad (6-21)$$

where c is the speed of light in a vacuum, k is a mode-coupling factor which equals 1.0 for negligible mode coupling (see clause 3.1.5.2) and 0.82 in the limit of random mode coupling (see clause 3.1.5.1).

If a polarimeter is used as the detection element, take as the final value of $\langle \Delta\tau \rangle$ the average of the values derived from the three normalized Stokes parameter responses. The resulting value is to be interpreted as an average over the wavelength range $\lambda_1 < \lambda < \lambda_2$.

6.1.4.4.1.2 Accuracy

The best accuracy is obtained by making $(\lambda_2 - \lambda_1)$ large enough to ensure that $E \gg 1$. This is especially important when there is random mode coupling (Figure 13-b) and less so otherwise (Figure 13-a). Values of E in the range of 7 to 40 are typical. When E is at the low end of this range, the percentage of uncertainties in both E and the PMD become large. At the upper end of the range, instrumental broadening may result in some adjacent peaks not being resolved.

Ideally, the scan window should be centred on the fibre's wavelength of use, and the window made wide enough to ensure that E is greater than about 10 for the maximum PMD value of interest (where pass/fail is an issue).

6.1.4.4.1.3 Peak identification

The identification of extrema in $R(\lambda)$ can be more difficult in the presence of noise or random mode coupling. This can be seen in the example of Figure 13-b. An algorithm with the following features is useful in identifying extrema:

- 1) A polynomial is fitted to several adjacent points of $R(\lambda)$ to provide a smoothed curve.
- 2) An extremum is defined as a point where the wavelength derivative of this smoothed curve changes sign.

Additional robustness can be built into the peak identification algorithm if needed.

6.1.4.4.1.4 Spectral resolution

To ensure that all features in the optical spectrum are adequately resolved, the spectral resolution $\Delta\lambda$ should satisfy:

$$\Delta\lambda/\lambda < (8\nu\Delta\tau)^{-1} \quad (6-22)$$

where ν is the optical frequency. $\Delta\lambda$ is the instrumental spectral width or the wavelength step size, whichever is larger. For λ in the vicinity of 1 550 nm, Equation 6-22 reduces to the condition that $\Delta\lambda$ in nanometres should be less than the reciprocal of $\Delta\tau$ in picoseconds.

6.1.4.4.2 Fourier analysis

6.1.4.4.2.1 Overview

In this method, a Fourier analysis of $R(\lambda)$, usually expressed in the domain of optical frequency, ν , is used to derive PMD. The Fourier transform transforms this optical frequency domain data to the time domain. The Fourier transform yields direct information on the distribution of light arrival times, $\Delta\tau$. This data is post-processed as described below to derive the expected PMD, $\langle \Delta\tau \rangle$, for the fibre under test. This method is applicable to fibres with negligible or random mode coupling (refer to clauses 6.1.4.4.2.4 and 6.1.4.4.2.5, respectively).

6.1.4.4.2.2 Data preprocessing and Fourier transformation

To use this method, the Fourier transform normally requires equal intervals in optical frequency so that $R(\lambda)$ data is collected (as described in clause 6.1.4.3) at λ values such that they form equal intervals in the optical frequency domain. Alternatively, data taken at equal λ intervals may be fitted (e.g., by using a cubic spline fit) and interpolation used to generate these points, or more advanced spectral estimation techniques used. In each instance, the ratio $R(\lambda)$ at each λ value used is calculated using Equations 6-19 or 6-20 as appropriate.

Zero-padding or data interpolation and DC level removal may be performed on the ratio data, $R(\lambda)$. Windowing the data may also be used as a preconditioning step before the Fourier transform. The Fourier transformation is now carried out to yield the amplitude data distribution $P(\delta\tau)$ for each value of $\delta\tau$.

6.1.4.4.2.3 Transform data fitting

Fourier transformed data at zero $\delta\tau$ has little meaning since, unless carefully removed, DC components in $R(\lambda)$ may be partially due to insertion loss of the analyser, for example. When the DC level is not removed, up to two data points are generally bypassed (not used) in any further calculations. A variable, j , is defined so that the "first valid bin" above zero $\delta\tau$ that is included in calculations corresponds to $j = 0$.

In order to remove measurement noise from subsequent calculations, $P(\delta\tau)$ is compared to a threshold level T_1 , typically set to 200% of the RMS noise level of the detection system. It is now necessary to determine whether the fibre is negligibly or randomly mode coupled.

If it is found that the first X valid points of $P(\delta\tau)$ are all below T_1 , this indicates that $P(\delta\tau)$ must have discrete spike features characteristic of negligibly coupled fibres. Unless zero-padding is used in the Fourier analysis, $X = 3$. In that case, the value of X can be determined from 3 times the number of original data points divided by the total length of array after zero-padding. Use clause 6.1.4.4.2.4 to calculate PMD. If this is not the case, proceed to calculate PMD using clauses 6.1.4.4.2.5 or 6.1.4.4.2.6.

6.1.4.4.2.4 PMD calculation for fibres with negligible mode coupling

For a negligibly coupled fibre (e.g., a high birefringence fibre) or for a birefringent component, $R(\lambda)$ resembles a chirped sine wave (Figure 13-a). Fourier transformation will give a $P(\delta\tau)$ output containing a discrete spike at a position corresponding to the relative pulse arrival time, $\delta\tau$, the centroid of which is the PMD value $\langle\Delta\tau\rangle$.

To define the spike centroid $\langle\Delta\tau\rangle$, those points where $P(\delta\tau)$ exceeds a second predetermined threshold level T_2 , typically set to 200% of the RMS noise level of the detection system, are used in Equation 6-23:

$$\langle\Delta\tau\rangle = \frac{\sum_{e=0}^{M'} [P_e(\delta\tau)\delta\tau_e]}{\sum_{e=0}^{M'} [P_e(\delta\tau)]} \quad (6-23)$$

where $M' + 1$ is the number of data points of P within the spike which exceed T_2 . $\langle\Delta\tau\rangle$ in Equation 6-23 is typically quoted in picoseconds. If the device under test is a fibre of length L , the PMD coefficient may be calculated using clause 3.1.5.2. If no spike is detected (i.e., $M' = 0$), then PMD is zero. Other parameters such as the RMS spike width or spike peak value may be reported.

If the device under test contains one or more birefringent elements, more than one spike will be generated. For a number n concatenated fibres/devices, $2^{(n-1)}$ spikes will be obtained.

6.1.4.4.2.5 PMD calculation for fibres with random mode coupling

In instances of random mode coupling, $R(\lambda)$ becomes a complex waveform similar to Figure 13-b, the exact characteristics being based on the actual statistics of the coupling process within the fibre or cable. The Fourier transformed data now becomes a distribution $P(\delta\tau)$ representing the autocorrelation of the probability distribution of light pulse arrival times, $\delta\tau$, in the fibre.

Counting up from $j = 0$, determine the first point of P which exceeds T_1 , and which is followed by at least X data points which fall below T_1 . This point represents the last significant point in (i.e., the "end" of) the distribution $P(\delta\tau)$, for a randomly mode-coupled fibre, that is not substantially affected by measurement noise. The $\delta\tau$ value for this point is denoted $\delta\tau_{last}$, and the value of j at $\delta\tau_{last}$ is denoted

M'' . This fibre is randomly mode coupled. The square root of the second moment, σ_R , of this distribution defines the fibre PMD $\langle \Delta\tau \rangle$, and is given by:

$$\langle \Delta\tau \rangle = \sigma_R = \sqrt{\frac{\sum_{j=0}^{M''} [P_j(\delta\tau) \delta\tau_j^2]}{\sum_{j=0}^{M''} [P_j(\delta\tau)]}} \quad (6-24)$$

The $\langle \Delta\tau \rangle$ value given by Equation 6-24 is typically quoted in picoseconds and normalized to picoseconds per root kilometre using clause 3.1.5.1. An example of the Fourier transform output obtained in a 25 km fibre with random mode coupling is shown in Figure 14.

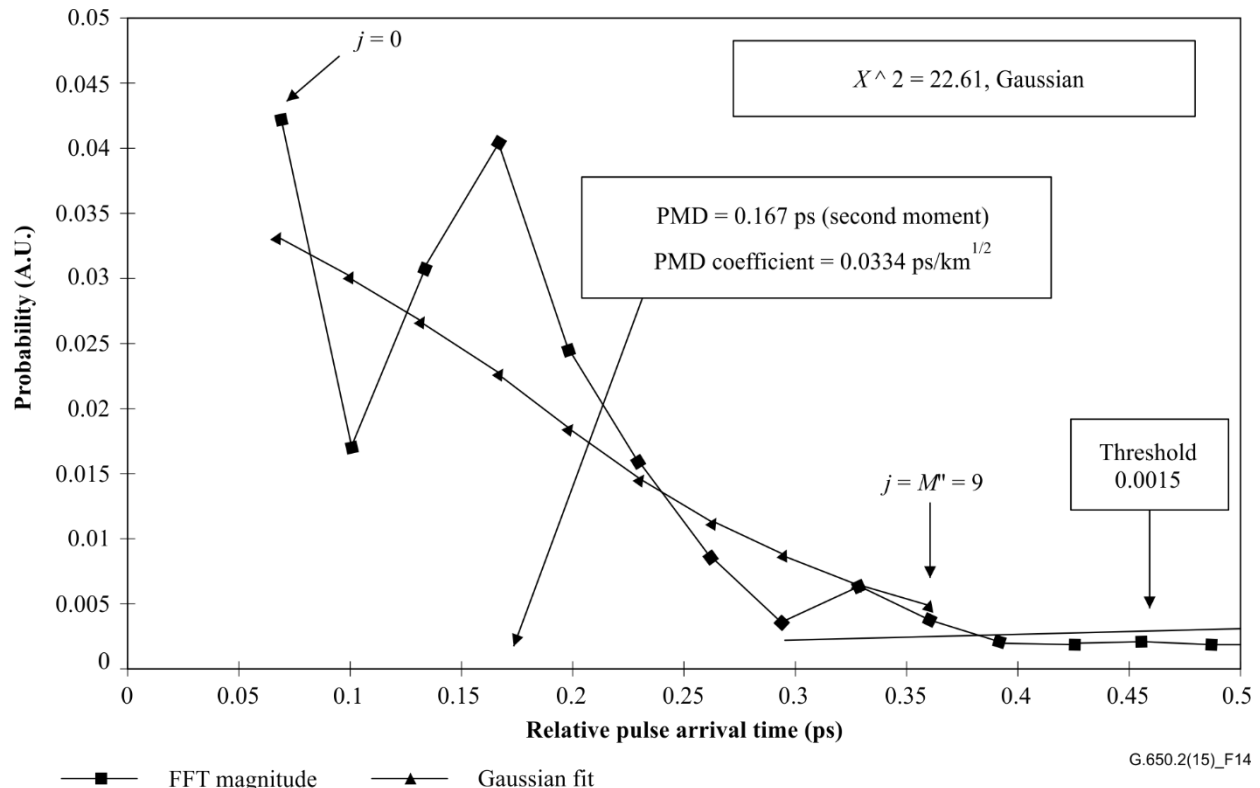


Figure 14 – PMD using Fourier analysis

6.1.4.4.2.6 PMD calculation for mixed coupling fibre systems

There may be instances where both negligibly coupled fibre or components and randomly coupled fibre(s) are concatenated to form the system under test. In this case, both centroid determination (clause 6.1.4.4.2.4) and the second moment derivation (clause 6.1.4.4.2.5) may be required. Note that spikes in $P(\delta\tau)$ may only be determined beyond the $\delta\tau_{last}$ computed.

6.1.4.4.2.7 Spectral range

For randomly coupled fibres, sufficient spectral range must be used to form the spectral ensemble (average) with sufficient precision. The statistical uncertainty may be minimized by using the widest possible spectral range (e.g., at least 200 nm). The precision required and therefore spectral range must be specified prior to the measurement. The maximum usable range is limited by the fibre cut-off wavelength (1 270 nm or below) at the short (λ_1) end, and by the detector responsivity roll-off at the high (λ_2) end (e.g., 1 700 nm).

In addition, very low $\delta\tau$ values will give very long periods in $R(\lambda)$, and the spectral range λ_1 to λ_2 must cover at least two complete cycles. The spectral range covered defines the smallest $\delta\tau$ value that can be resolved in $P(\delta\tau)$, $\delta\tau_{min}$:

$$\delta\tau_{\min} = \frac{2\lambda_1\lambda_2}{(\lambda_2 - \lambda_1)c} \quad (6-25)$$

where the factor 2 is introduced to allow for the fact that two data points in P at and adjacent to zero are generally ignored (see clause 6.1.4.4.2.3). For example, for $\lambda_1 = 1\ 270\ \text{nm}$, $\lambda_2 = 1\ 700\ \text{nm}$, $\delta\tau_{\min} = 0.033\ \text{ps}$.

For negligibly coupled high PMD fibres with ratio data $R(\lambda)$ resembling Figure 13-a, the requirement for spectral averaging described above may be relaxed, and the spectral range reduced [e.g., $(\lambda_2 - \lambda_1) \sim 30\ \text{nm}$] in order to allow variation of PMD with wavelength to be examined.

6.1.4.4.2.8 Wavelength step size and spectral resolution

To ensure that all features (frequencies) in $R(\lambda)$ are adequately resolved, the monochromator step size, expressed in the optical frequency domain ($\Delta\nu$) must be a factor of two smaller than the oscillation frequency corresponding to the maximum $\delta\tau$ measured (Nyquist condition):

$$\delta\tau_{\max} = 1/(2 \cdot \Delta\nu) \quad (6-26)$$

If, from the Fourier transform, it is evident that significant energy is present near to $\delta\tau_{\max}$ [i.e., that $R(\lambda)$ appears to be "aliased"], it will be necessary to reduce the step size $\Delta\nu$ (if possible) and repeat the measurement.

The monochromator spectral linewidth (resolution) expressed in optical frequency units is generally equal to or smaller than the smallest $\Delta\nu$ value to be used (corresponding to the largest $\delta\tau$ value to be measured).

For example, for $\delta\tau_{\max} = 1.34\ \text{ps}$, a monochromator linewidth of 3 nm at 1 550 nm ($\Delta\nu = 374\ \text{GHz}$) is typical.

6.1.4.4.3 Cosine Fourier analysis

This analysis is based on the observation that the cosine Fourier transform of the spectrum emitted from the analyser is the fringe pattern of the interferogram. The difference between fringe patterns generated by the analyser being set at two orthogonal settings is the cross-correlation function. For an infinite spectrum into the analyser, the autocorrelation function would have zero width. In practice, the finite source spectrum in the optical frequency domain (finite linewidth) acts as a windowing function which produces a non-zero autocorrelation function width in the time domain.

The analysis of the squared cross-correlation and autocorrelation functions found in the GINTY analysis of clause 6.1.3 shows that the difference in squared RMS widths of these functions is proportional to the square of the spectrally weighted RMS (by squared power) of the DGD values. (See Equation 6-18.)

The result is independent of the spectral shape which means that the details of the windowing function are fully taken into account. It is also independent of the degree of mode coupling, which means that no changes in algorithm are needed to treat the different regimes.

The result is limited by the spectral width and optical frequency increment that is measured. As the PMD increases, the frequency increment must be decreased. At some limit it would be more practical to use the GINTY.

The analysis reports the PMD_{RMS} metric. If random mode coupling is found, the result can be converted to PMD_{AVG} using Equation 3-3.

6.1.4.4.3.1 Overview

The measurement of the powers emitted from the analyser set at two orthogonal settings is required. The ratio, R , associated with Equation 6-20 is modified to:

$$R(v) = \frac{P_A(v) - P_B(v)}{P_A(v) + P_B(v)} \quad (6-27)$$

where $v = c/\lambda$ is the optical frequency, in terahertz.

If a polarimeter is used, the three normalized output Stokes vector elements are equivalent to three independent normalized ratios equivalent to that represented by Equation 6-27. Each Stokes vector element is the difference in powers between orthogonal analyser settings. The three elements are different in that the base settings are also orthogonal.

The data are multiplied by a windowing function, $W(v)$, that goes to zero smoothly at the edges. Both $R(v)W(v)$ and $W(v)$ are put into arrays with zero padding at lower, unmeasured frequencies. Fast cosine Fourier transforms (FCFTs) are applied to each array to obtain the time domain fringe envelopes, $r(t)w(t)$ and $w(t)$. These are squared to obtain the squared cross-correlation and autocorrelation envelopes, E_x^2 and E_0^2 , respectively. When multiple ratio functions (N) are available from different combinations of input polarizer setting and base analyser settings (or different Stokes output vector elements), using for instance I/O SOP scrambling, form the mean square envelopes as:

$$\bar{E}_x^2 = \frac{1}{N} \sum_i E_{xi}^2 \quad \bar{E}_0^2 = \frac{1}{N} \sum_i E_{0i}^2 \quad (6-28)$$

Using the RMS calculation of clause I.2, calculate the RMS widths, σ_x and σ_0 of these two functions. The PMD_{RMS} value is calculated as:

$$\text{PMD}_{\text{RMS}} = \left[\frac{3}{2} (\sigma_x^2 - \sigma_0^2) \right]^{1/2} \quad (6-29)$$

It is related to the spectrally weighted (by squared window value) RMS of the DGDs as:

$$\langle \text{PMD}_{\text{RMS}} \rangle = \frac{\int \Delta\tau^2(v) W^2(v) dv}{\int W^2(v) dv} \quad (6-30)$$

The expected value operator is with respect to random I/O SOPs.

6.1.4.4.3.2 Details

This clause explains some of the details with respect to the measured frequency window, the frequency increment, Δv , frequency shifting, and the result of the FCFT. An example of a FCFT algorithm may be found in [b-Press 1992].

The data must be available in uniform frequency increments. The number of data points, including zero pad values, must be $1 + 2^k$, with k an integer.

If the n_m data measured data points are not taken in uniform frequency increments, they may be fitted to a polynomial such as a spline for interpolation. A cubic spline with $n_m - 3$ uniform segments will fit all the data perfectly and allow interpolation.

Given that the measured data are bounded by $v_{\min M}$ and $v_{\max M}$ and the fact that the minimum optical frequency is well above zero, the application of frequency shifting can be used to reduce the size of the arrays that are processed. The boundaries of the frequencies used in the calculation array can be selected by any choice of n such that:

$$v_{\max} \frac{n-1}{n} = v_{\min} \leq v_{\min M}, \quad v_{\max} = v_{\max M} \quad (6-31)$$

and n is a positive integer.

The frequency values less than the measured frequency are filled with zeros.

Following the FCFT, the array will contain the time domain fringe pattern from times of 0 to $t_{\max} = \Delta t 2^k$, where the time increment, Δt , is given as:

$$\Delta t = \frac{n}{2v_{\max}} = \frac{1}{2(v_{\max} - v_{\min})} \quad (6-32)$$

The fringe pattern that would be obtained from interferometry extends to negative time values as well as positive time values. The value at a given negative time is equal to the value at the positive time. The function is even and symmetric about zero. This can lead to simplifying the calculation of RMS since time zero is known.

The selection of the frequency shift should be done keeping in mind that the RMS width calculation needs some time domain values that are less than the minimum PMD_{RMS} that is measurable.

The frequency increment, Δv , is also related to the number of points sampled, the frequency shift and the maximum PMD_{RMS} that is to be measured. It is given as the following, along with the constraint as:

$$\Delta v = \frac{v_{\max} - v_{\min}}{2^k} \leq \frac{1}{24\text{PMD}_{\text{RMS}-\max}} \quad (6-33)$$

The constraint in Expression 6-33 is consistent with Equation 6-22. The spectral width of the filtered source should be half of this value. When the actual scan is done in equal wavelength increments, the wavelength increment at the lower end of the range should be consistent with the constraint of Equation 6-33.

The windowing function, $W(v)$, can technically be any function, including a square function. The function that is chosen should be one that minimizes the value of σ_0 . Functions that do this proceed to zero at the edges in a continuous way and should also have the first derivative proceed to zero at the edges. This will minimize the ringing that can increase σ_0 .

6.1.4.4.3.3 Examples

Table 1 shows a sample calculation spreadsheet. The wavelength extrema and k are centred. For each of several possible frequency shift values, n , the other parameters are calculated. PMD_{\min} is calculated as $3\Delta t$. The effective shift in terms of $\Delta\lambda$ at the lower wavelength limit is also presented. Clearly there are trade-offs, depending on the range of PMD_{RMS} values that are to be measured. In general, the broader the wavelength range and the smaller the frequency increment, the better.

Table 1 – Cosine transform calculations

<i>c</i> :	299792.5 nm/ps					
<i>k</i> :	11					
<i>npt</i> :	2 048 (Note)					
Wavelengths (nm)						
Max	1 700					
Min	1 300					
Frequencies (THz)						
	230.609 6					
	176.348 5					
Frequency shift						
<i>n</i>	ν_{\min} (THz)	Δt (ps)	$\Delta\nu$ (THz)	PMD_{\min} (ps)	PMD_{\max} (ps)	$\Delta\lambda$ (nm)
1	0	0.002 168	0.112 602	0.006 504	0.370 034	0.635 076
2	115.304 807 7	0.004 336	0.225 205	0.013 009	0.185 017	1.270 772
3	153.739 743 6	0.006 504	0.337 807	0.019 513	0.123 345	1.907 090
4	172.957 211 5	0.008 673	0.450 409	0.026 018	0.092 508	2.544 031
5	184.487 692 3	0.010 841	0.563 012	0.032 522	0.074 007	3.181 596
6	192.174 679 5	0.013 009	0.675 614	0.039 027	0.061 672	3.819 785
7	197.665 384 6	0.015 177	0.788 216	0.045 531	0.052 862	4.458 599
8	201.783 413 5	0.017 345	0.900 819	0.052 036	0.046 254	5.098 039

NOTE – *npt* is the number of points to be cosine transformed, and is equal to 2^k . The number of points in the test is usually less than this and the space not filled with actual data are filled with zero.

The following illustrates the results for what might be obtained from a fibre with $\text{PMD}_{\text{RMS}} = 0.2$ ps. The mean cross-correlation and mean autocorrelation envelopes from a single scan using a windowing function that is Gaussian with a standard deviation of 23 nm are shown in Figure 15. The result is from a simulation of a fibre with ideal random mode coupling. The measured result for this simulation was 0.185 ps.

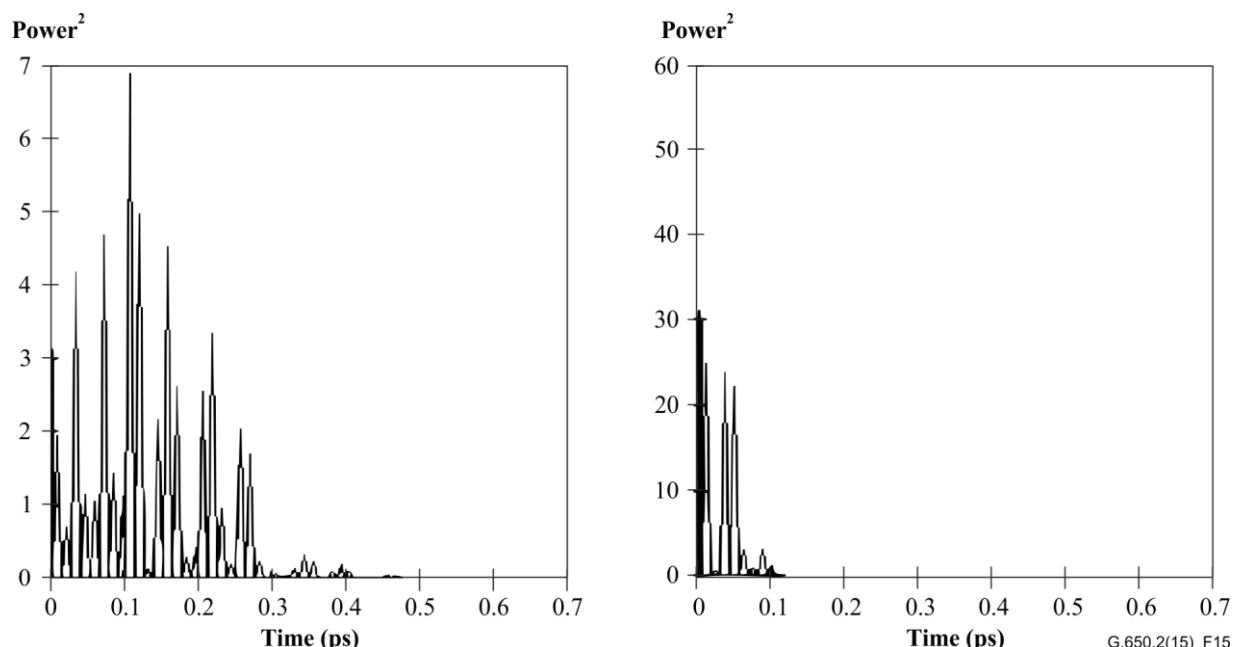


Figure 15 – Cross-correlation and autocorrelation functions

6.1.4.5 Presentation of the results

The following details shall be presented:

- a) Identification of the fibre or cable measured.
- b) Test length.
- c) PMD (typically in picoseconds). If the degree of mode coupling is known, the PMD coefficient may be given in picosecond per kilometre (negligible mode coupling) or picosecond per root kilometre (random mode coupling).
- d) The wavelength range over which the measurement was performed, and the wavelength or frequency step size.
- e) The physical configuration of the fibre or cable sample.
- f) Mode-coupling type, e.g., deterministic, semi-random or random.
- g) When an average PMD has been obtained from repeated measurements of the sample, record the number of measurements performed.

6.2 Test methods for non-linear attributes

Under study.

Appendix I

Determination of PMD delay from an interferogram

(This appendix does not form an integral part of this Recommendation.)

This appendix presents two methods for the determination of the RMS width from fringe envelopes. These methods are mainly used for the interferometric method of measuring PMD. Clause I.1 is for an envelope with the autocorrelation peak present and is suitable for the TINTY analysis. Clause I.2 is for envelopes without this peak and is suitable for the GINTY analysis.

I.1 RMS calculation for TINTY

Figure I.1 shows a fringe envelope with an autocorrelation peak in the centre.

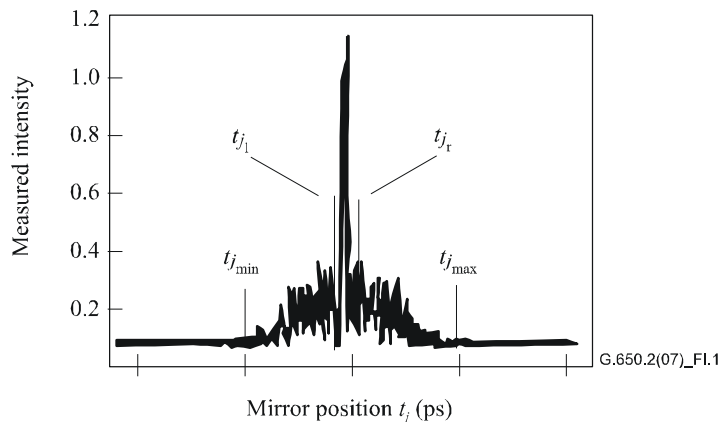


Figure I.1 – Parameters for interferogram analysis

Let \tilde{I}_j denote the measured intensity of the fringe envelope at increasing positions t_j , $j = 1 \dots N$, with $[t_j]$ in picoseconds.

Step 1 – Computation of the zero intensity \tilde{I}_0 and the noise amplitude Na

Definition: $N_5 = \text{round}(5N/100)$

$$\tilde{I}_0 = \frac{\sum_{j=1}^{N_5} (\tilde{I}_j + \tilde{I}_{N-j})}{2N_5} \quad (I-1)$$

$$X_2 = \frac{\sum_{j=1}^{N_5} (\tilde{I}_j^2 + \tilde{I}_{N-j}^2)}{2N_5} \quad (I-2)$$

$$Na = \sqrt{X_2 - I_0^2} \quad (I-3)$$

Step 2 – Definition of the shifted intensity I_j

$$I_j := \tilde{I}_j - \tilde{I}_0 \text{ if } \tilde{I}_j - \tilde{I}_0 > 4Na \quad (\text{I-4})$$

$$I_j := 0 \text{ if } \tilde{I}_j - \tilde{I}_0 \leq 4Na \quad (\text{I-5})$$

Step 3 – Computation of the centre C of the interferogram

$$C = \frac{\sum_{j=1}^N t_j I_j}{\sum_{j=1}^N I_j} \quad (\text{I-6})$$

Step 4 – Removal of the central autocorrelation peak

Definition: $j_l :=$ the largest subscript j such that $C - t_j > \tau_c$ (I-7)

$j_r :=$ the smallest subscript j such that $t_j - C > \tau_c$ (I-8)

where τ_c is the source coherence time.

NOTE 1 – For cross-correlation interferograms, the following definition shall be applied:

$$j_r := j_l + 1 \quad (\text{I-9})$$

Step 5 – Computation of the second moment S of the interferogram

$$S = \frac{1}{2} \left\{ \sqrt{\frac{\sum_{j=1}^{j_l} (t_j - C)^2 I_j}{\sum_{j=1}^{j_l} I_j}} + \sqrt{\frac{\sum_{j=j_r}^N (t_j - C)^2 I_j}{\sum_{j=j_r}^N I_j}} \right\} \quad (\text{I-10})$$

Step 6 – Truncate the interferogram

Set j_{\min} to the largest subscript j such that $C - t_j > 2S$ (I-11)

Set j_{\max} to the smallest subscript j such that $t_j - C > 2S$ (I-12)

Step 7 – Computation of the second moment σ_ε of the truncated interferogram

$$\sigma_\varepsilon = \frac{1}{2} \left\{ \sqrt{\frac{\sum_{j=j_{\min}}^{j_l} (t_j - C)^2 I_j}{\sum_{j=j_{\min}}^{j_l} I_j}} + \sqrt{\frac{\sum_{j=j_r}^{j_{\max}} (t_j - C)^2 I_j}{\sum_{j=j_r}^{j_{\max}} I_j}} \right\} \quad (\text{I-13})$$

Step 8 – Computation of the σ of the Gaussian $\exp(-(t - C)^2 / 2\sigma^2)$ such that:

$$\sigma_\varepsilon = \frac{1}{2} \left\{ \sqrt{\frac{\int_{t_{j_{\min}}}^{t_{j_l}} (t - C)^2 \exp[-(t - C)^2 / 2\sigma^2] dt}{\int_{t_{j_{\min}}}^{t_{j_l}} \exp[-(t - C)^2 / 2\sigma^2] dt}} + \sqrt{\frac{\int_{t_{j_r}}^{t_{j_{\max}}} (t - C)^2 \exp[-(t - C)^2 / 2\sigma^2] dt}{\int_{t_{j_r}}^{t_{j_{\max}}} \exp[-(t - C)^2 / 2\sigma^2] dt}} \right\} \quad (\text{I-14})$$

Step 9 – Determination of PMD_{RMS} ($\Delta\tau^2$)^{1/2}

$$\text{PMD}_{\text{RMS}} = \langle \Delta\tau^2 \rangle^{1/2} = \sqrt{\frac{3}{4}\sigma} \quad (\text{I-15})$$

NOTE 2 – For appropriately measured interferograms, it can be shown that $\frac{\sigma_\varepsilon}{\sigma} \approx \sqrt{\frac{3}{4}}$.

I.2 RMS calculation for GINTY

The following algorithm results in a robust RMS width for either the composite square cross-correlation or autocorrelation envelopes using method D (GINTY).

The algorithm is iterative. For a given iteration, the full data array is divided into two sets: The central portion, M, containing the signal and the tails, T, which contain noise. Each iteration results in different definitions for these sets. The result converges when either the computed RMS width ceases to vary or when the set definitions stabilize. For an iteration, the number of data points in each set are denoted as N_M and N_T .

Let \tilde{I}_j denote the measured intensity of the envelope at increasing positions t_j (ps), (ps), $j = 1\dots N$.

The initial definition of the set T is the first and last 5% of the whole array.

Step 1 – Computation of the zero \tilde{I}_0

$$\tilde{I}_0 = \sum_{j \in T} \tilde{I}_j / N_T \quad (\text{I-16})$$

Step 2 – Definition of the shifted intensity I_j

$$I_j = \tilde{I}_j - \tilde{I}_0 \quad \text{all } N \quad (\text{I-17})$$

Step 3 – Computation of the centre C of the interferogram

$$C = \frac{\sum_{j \in M} t_j I_j}{\sum_{j \in M} I_j} \quad (\text{I-18})$$

Step 4 – Computation of the RMS width σ of the squared envelope

$$\sigma^2 = \frac{\sum_{j \in M} (t_j - C)^2 I_j}{\sum_{j \in M} I_j} \quad (\text{I-19})$$

Step 5 – Redefine the sets

Define M as the set of points for which $C - 4\sigma \leq t_j \leq C + 4\sigma$.

Define T as the rest of the points.

Step 6 – Repeat steps 1 to 5 until the results converge

$$\frac{\sigma_\varepsilon}{\sigma} \approx \sqrt{\frac{3}{4}}$$

Appendix II

Non-linear attributes

(This appendix does not form an integral part of this Recommendation.)

II.1 Background

Non-linear interactions between the signal and the silica fibre transmission medium begin to appear as optical signal powers and are increased to achieve longer span lengths at high bit rates. Consequently, non-linear fibre behaviour has emerged as an important consideration, both in high capacity systems and in long unregenerated routes. These non-linearities can be generally categorized as either scattering effects (stimulated Brillouin scattering and stimulated Raman scattering) or effects related to the Kerr effect, that is, the intensity dependence of the refractive index (self-phase modulation, cross-phase modulation, modulation instability, soliton formation and four wave mixing). A variety of parameters influence the severity of these non-linear effects, including fibre dispersion characteristics, the effective area of the fibre, the number and spacing of channels in multiple channel systems, overall unregenerated system length, the degree of longitudinal uniformity of the fibre characteristics, as well as signal intensity and source linewidth.

II.2 Effective area (A_{eff})

Effective area is a parameter that is closely related to optical fibre non-linearities that will affect the transmission quality of the optical fibre systems, especially in long-haul optically amplified systems.

Effective area A_{eff} is defined as follows:

$$A_{\text{eff}} = \frac{2\pi \left[\int_0^{\infty} I(r) r dr \right]^2}{\int_0^{\infty} I(r)^2 r dr} \quad (\text{II-1})$$

where $I(r)$ is the field intensity distribution of the fundamental mode of the fibre at radius r . The integration of Equation II-1 is carried out over the entire cross-sectional area of the fibre. For example, if we make a Gaussian approximation such that:

$$I(r) = \exp(-2r^2/w^2) \quad (\text{II-2})$$

where $2w$ is the mode field diameter (MFD), then Equation II-1 can be analytically integrated and gives:

$$A_{\text{eff}} = \pi w^2 \quad (\text{II-3})$$

The Gaussian approximation is accurate for ITU-T G.652 and ITU-T G.654 step-index fibres near the LP₁₁ cut-off, but for ITU-T G.652 and ITU-T G.654 fibres at much longer wavelengths, and in the case of ITU-T G.653 dispersion shifted fibres, A_{eff} cannot be accurately estimated from Equation II-3.

A more general but empirical relationship between A_{eff} and w is [b-Namihira 1994]:

$$A_{\text{eff}} = k\pi w^2 \quad (\text{II-4})$$

where k is a correction factor.

II.3 Correction factor k

In the experiment, the MFD was measured by the variable aperture test method. From the far-field pattern (FFP) of the output optical power $P(r)$, it was then possible to calculate the near-field pattern (NFP) using an inverse Hankel transformation. A_{eff} is then derived from the NFP by using Equation II-1.

The correction factor k in Equation II-4 depends on the wavelength and on fibre parameters, such as refractive index profiles, MFD and zero-dispersion wavelength.

Figure II.1 shows examples of measured wavelength dependence of MFD and A_{eff} for ITU-T G.652 and ITU-T G.653 fibres in the 1 200–1 600 nm wavelength regions. Figure II.2 gives examples of calculated and measured wavelength dependence of MFD, A_{eff} , and the correction factor k for ITU-T G.652, ITU-T G.653 and ITU-T G.654 fibres in this same wavelength range.

The ranges of the correction factor k for these examples are summarized in Table II.1.

For other fibre designs that may be developed for optical submarine and wavelength division multiplexing (WDM) applications, the relationship of A_{eff} to w may vary, and should be determined using Equation II-1.

Figure II.3 shows the wavelength dependence of A_{eff} for ITU-T G.653 (dispersion-shifted single-mode fibre; DSF) and ITU-T G.655 (NZ-DSF) fibres in the 1 520–1 580 nm wavelength range for WDM applications.

The average k values and standard deviation were found to be around $0.953 \pm .005$ for the ITU-T G.653 fibres, and $1.09 \pm .070$ for the ITU-T G.655 fibres.

Table II.1 – Summary of correction factor k of A_{eff} and MFD ($= 2w$) for ITU-T G.652, ITU-T G.653 and ITU-T G.654 fibres based on the examples in Figure II.2

Fibre types	Wavelength λ	
	~ 1 310 nm	~ 1 550 nm
ITU-T G.652	0.970 ~ 0.980 (Note)	0.960 ~ 0.970
ITU-T G.654	...	0.975 ~ 0.985 (Note)
ITU-T G.653	0.940 ~ 0.950	0.950 ~ 0.960 (Note)
NOTE – Optimum wavelength range.		

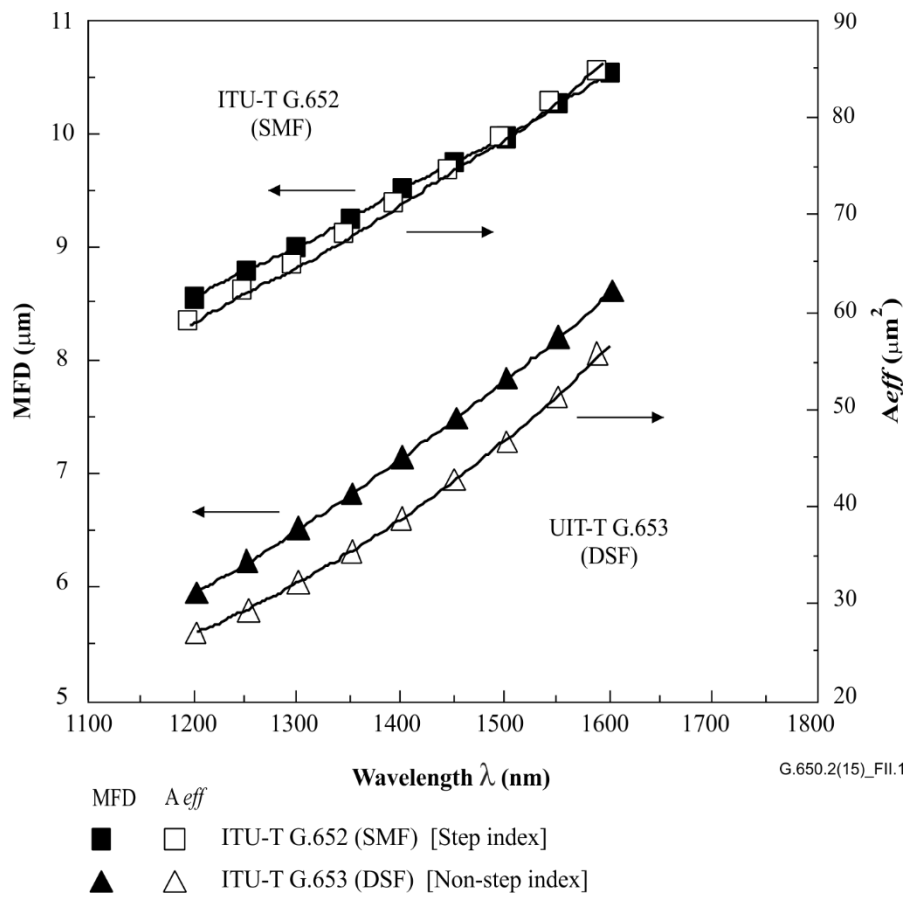


Figure II.1 – Example of measured wavelength dependence of A_{eff} and MFD ($= 2w$) of ITU-T G.652 and ITU-T G.653 fibres

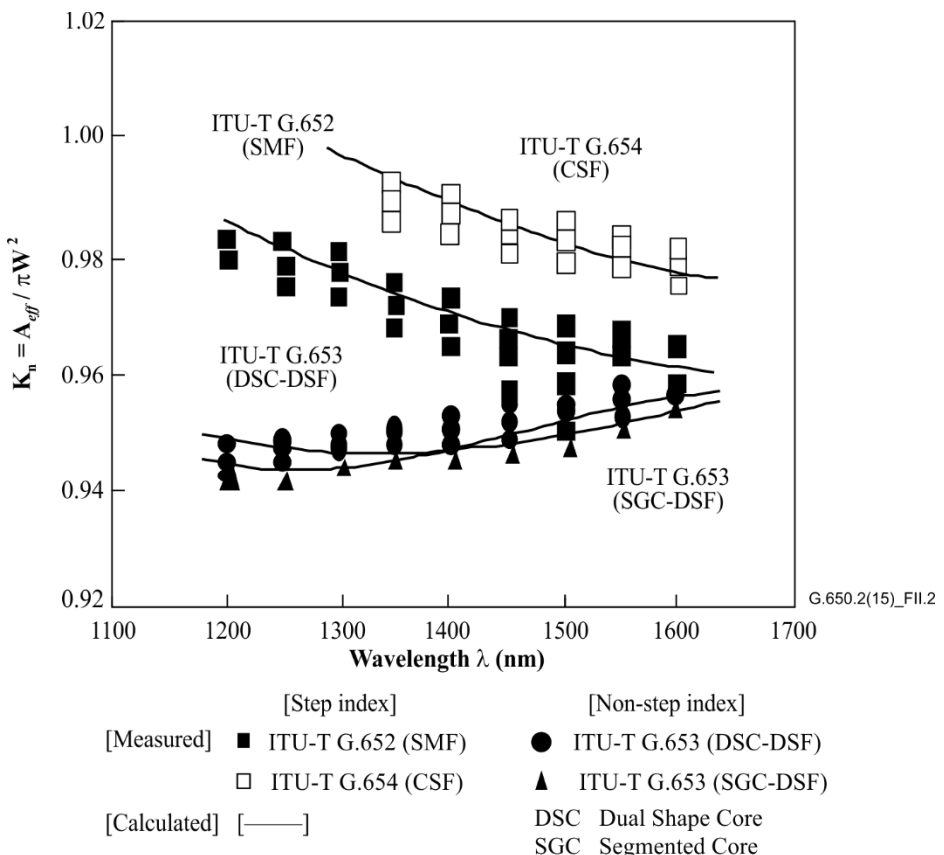


Figure II.2 – Example of calculated and measured wavelength dependence of correction factor k for ITU-T G.652, ITU-T G.653 and ITU-T G.654 fibres

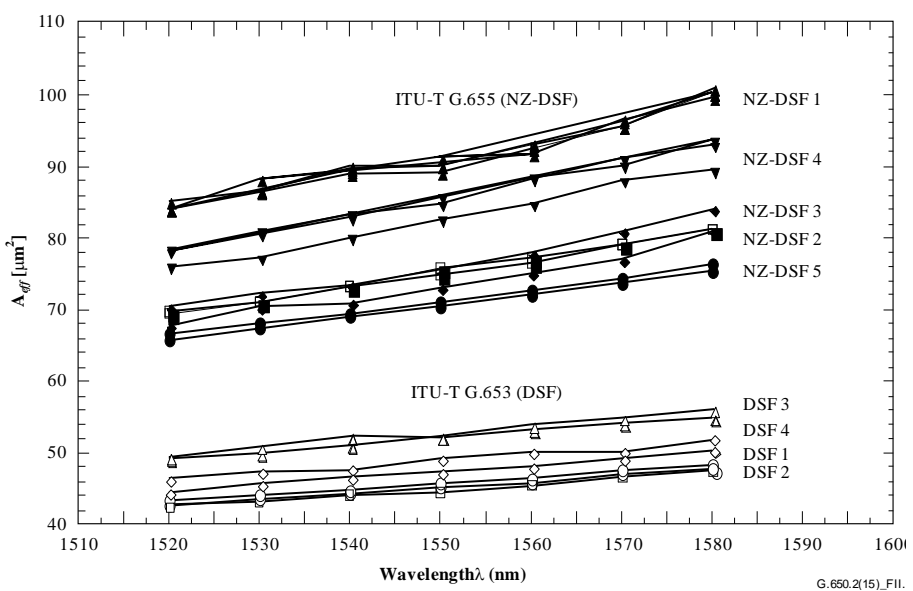


Figure II.3 – Example of measured λ dependence of A_{eff} for ITU-T G.653 and ITU-T G.655 fibres

II.4 Non-linear coefficient (n_2/A_{eff})

For particularly intense fields, the refractive index of optical fibres is dependent on optical intensity inside the fibres, and can be expressed as:

$$n = n_0 + n_2 I \quad (\text{II-5})$$

where n is the refractive index, n_0 the linear part of the refractive index, n_2 the non-linear refractive index and I the optical intensity inside the fibres.

The non-linear coefficient is defined as n_2/A_{eff} . This coefficient plays an important role in evaluating the system performance degradation due to non-linearities when high-power density systems are used.

Methods for measuring the non-linear coefficient are under study.

II.5 Stimulated Brillouin scattering

In a lightwave communication system using an optical source with a narrow linewidth, significant optical power may be transferred from a forward-propagating signal to a backward-propagating signal when the stimulated Brillouin scattering (SBS) power rating of the optical fibre is exceeded. In SBS, the forward-propagating light is scattered from acoustic phonons. Phase matching (or momentum conservation) dictates that the scattered light preferentially travels in the backward direction. The scattered light is downshifted (or Brillouin-shifted) by approximately 11 GHz at 1 550 nm.

II.5.1 Definitions and measurement overview

Several possible definitions of SBS power rating are provided as the input power level at which "substantial" backscatter occurs is not unique. This has been recognized previously, see for example [b-Smith 1972] and [b-Kobyakov 2002], where various terms and definitions have been used to quantify the SBS phenomenon (SBS threshold, SBS critical power, etc.). The common concept among these, however, is that the input power at which SBS becomes important is in the regime where the backscatter power begins to increase rapidly. Because of the exponential increase in backscatter power, the range of input powers in this regime is rather narrow [b-Kobyakov 2002], so all definitions give similar (though not identical) results.

Two SBS power rating definitions are given: one accounting for the rate of increase of the backscatter power, the other relating the backscatter power level to the input power level. These definitions differ in ease of use and visualization, immunity to noise and extraneous reflection, and consistency with theoretical work in the field.

II.5.1.1 Definitions

- A: The input power at which the rate of increase of the reflected power (with input power) is highest or accelerated maximally.
- Option 1 – The input power where the second derivative of the reflected power (mW/mW)² is maximum.
 - Option 2 – The input power where the second derivative of the transmitted power (mW/mW)² is minimum.
 - Option 3 – The input power where the first derivative of the reflected power (dBm/dBm) is maximum.
- B: The input power at which the reflected power equals 4% of the input power.

II.5.1.2 Measurement overview

The measurement is conducted by varying the input power into the fibre under test, usually to quite large power levels and usually at equal increments of power as represented by dBm. Using suitable optics at the input end, the reflected power can be measured at the same input powers. The transmitted power can also be measured. In all cases, the reflection from the far end of the fibre must be eliminated to prevent second order SBS interactions.

II.5.2 Apparatus

Figure II.4 shows a typical measurement set-up that can allow the measurement of input, reflected and transmitted power. The text following indicates some of the requirements. For measurements using only transmitted power, some elements are not required.

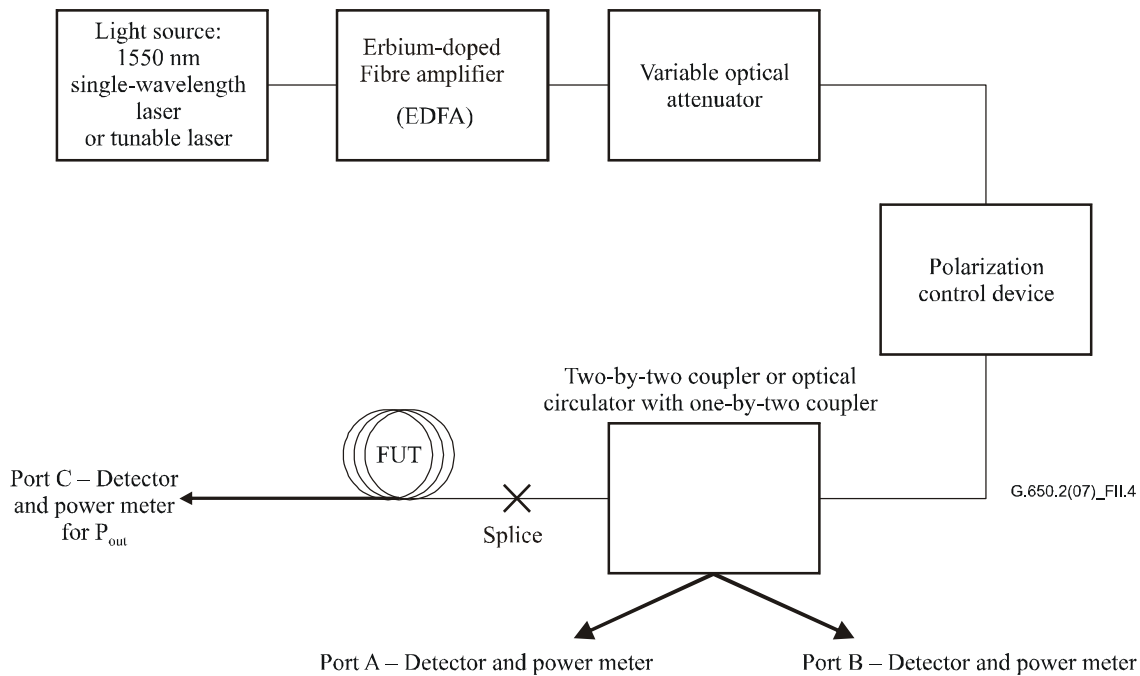


Figure II.4 – Typical SBS power rating measurement set-up

II.5.2.1 Light source

The light source shall be a narrow-band laser or tunable laser in the 1 550 nm region with the following characteristics:

- Sufficient power to produce adequate SNR through the erbium-doped fibre amplifier (EDFA).
- Optical frequency stable over the measurement period to within 20 kHz.
- Spectral width (FWHM) less than 200 kHz, with no significant delay line.
- DoP greater than 99%.
- Stable polarization state (SOP) over the duration of the test. This may be verified by monitoring port A.

II.5.2.2 Erbium-doped fibre amplifier (EDFA)

Depending on the length of the fibre under test, its sensitivity to SBS, and the SBS power rating definition that will be employed in analysis of the data, high powers can be required of the EDFA (15 dBm or more). The EDFA can contribute ASE which can reduce the SBS effects as well as induce depolarization. The SNR of the combination of source laser and EDFA is inversely proportional to the source laser power, but the relationship also depends on the details of the particular EDFA used. The SNR can be calculated from the output of an optical spectrum analyser for various source power levels. The source power shall be sufficiently large that the SNR is in excess of 17 dB. This can be achieved by controlling the EDFA pump power or alternatively by the provision of a bandpass filter.

The combination of source power and EDFA shall be stable to within 0.05 dBm over the period of the measurement.

The EDFA normally includes isolators. If it does not, isolators must be added. Care must be taken that EDFA performance is not degraded by inadequate isolation from large SBS backscatter.

II.5.2.3 Variable optical attenuator (VOA)

The power of the light that is inserted in the FUT is controlled with the VOA. The VOA should be capable of a range of approximately 20 dB with 0.1 dB increments. The measurement of a reference length removes the need for an absolute calibration of the VOA or its linearity.

II.5.2.4 Polarization control device

The polarization control device, which is optional, allows the power to the FUT to be optimized. It also allows for monitoring for changes in the state of polarization of the source during the course of a measurement. The power optimization results from the possible presence of small amounts of polarization-dependent loss in the other optical elements. Variation in the power monitored at port A gives an indication that the state of polarization of the source has changed.

II.5.2.5 Two-by-two coupler or optical circulator with one-by-two coupler

This device should allow most of the total output power to go into the FUT and a fraction, e.g., 5% or 1%, into port A. This device also allows the measurement of the reflected power at port B. If data analysis is to be performed using definition A then absolute calibration of this device is not required, but should be considered for certain experiments.

When calibration is completed, the actual measured power values (dBm) are adjusted by constants so that the adjusted powers are representative of the powers going through the pigtail fibre just after the coupler.

If a circulator with a one-by-two optical coupler is used, there can be fewer problems with light reflected back into the EDFA.

For either implementation, the linearity of the path from the end of the FUT to port B must be verified to be within 0.04 dB per dB. Non-linearities in excess of this value can place an upper limit on the measurement capability.

II.5.2.6 Pigtail and splice following the coupler/circulator

The pigtail following the coupler should be of sufficient length to allow repeated splices. The splice itself should be either a fusion splice or an angled cleave connector to eliminate reflections.

II.5.2.7 Fibre termination at port C

The fibre end is inserted into the power meter at port C in two situations:

- a) when the reference length is measured;
- b) when the transmitted power through the full length is measured (P_{out}).

Measurement of the transmitted power through the full length of the fibre is only required when using definition A, option 2. Certain experiments may involve this measurement even when other definitions are used. When the transmitted power is measured, an angle cleave of approximately 8° is recommended to prevent reflections that can affect the results measured at port B.

When no full length transmitted power measurements are required, deploy the far end of the FUT around a sufficiently small diameter mandrel or tight pin array to ensure that light is substantially stripped from the fibre before reaching the end.

Because end reflections can impair SBS power rating measurements using any of the definitions, it is recommended that the Rayleigh backscatter level (reflected power at very low input power) be examined before taking SBS data. ITU-T G.652 fibre of length greater than 20 km generally has a Rayleigh backscatter roughly 33 dB below the input power level. If higher levels than expected of Rayleigh backscatter are measured, the optical termination at the far end of the fibre must be improved.

The actual power launched into the full length fibre is measured by cutting off a section of approximately 2 m in length after the splice. The range of powers is then scanned again. As a result of the air/glass interface, there is a certain amount of light that is reflected (Fresnel reflection) that depends on the cleave angle of the fibre end. To control the amount of light lost due to Fresnel reflection to a constant 0.14 dB, cleave angles substantially less than 1° are recommended.

II.5.2.8 Power detectors

The power detectors at ports A, B and C should be calibrated according to [b-IEC 61315]. The absolute accuracy of the result using definition A is independent of the absolute accuracies of the detectors at ports A and B.

In addition to the absolute accuracy, the linearity of the meters, particularly those at ports B and C, should be verified to be within 0.04 dB per dB over the intended range of use.

II.5.2.9 General

The various connections throughout the system should either be fusion splices or angled connectors to avoid reflections.

The housing for the system should be opaque to avoid the possibility of high-power light escaping. The system should include a fail-safe mechanism or warning to prevent light in excess of 10 dBm (10 mW) from being emitted into the air in the path from the coupler to the FUT (either full length or reference measurement). This can be accomplished with the use of the power detected at port A.

II.5.3 Procedure

This procedure is to be applied to cabled or uncabled fibre. There is some evidence that the manner of deployment may affect the measured results. All measurements should be made at standard room temperature (20°C).

II.5.3.1 Procedure for reflected power measurement

- Set the VOA to a minimum output power.
- Fusion splice the input end of the fibre to the system and terminate the far end with a small diameter mandrel or pin array to eliminate the end reflection.
- Scan the VOA and take the reflected power readings from port B. Power readings from port A may be used to verify consistency of input power through the scan. Return the VOA to minimum power.
- Optionally, remove the termination device from the far end, prepare an 8° endface, and complete the VOA scan again to obtain transmitted power through port C. Return the VOA to minimum power.
- Cut the fibre under test to approximately 2 m from the connection at the source end. Prepare a flat endface to ensure maximum Fresnel reflection. Attach this end to port C.
- Scan the VOA again to obtain the measured input power through port C. Return the VOA to minimum power.
- The power values are normally reported in dBm. Make any adjustments for calibration factors associated with the coupler or circulator.

II.5.3.2 Procedure for transmitted power only

- Set the VOA to a minimum output power.
- Fusion splice the input end of the fibre to the system and terminate the far end to port C using an index-matching connection to minimize the far-end reflection interaction with the SBS process.
- Scan the VOA and take the transmitted power readings from port C. Power readings from port A may be used to verify consistency of input power through the scan. Return the VOA to minimum power.
- Cut the fibre under test to approximately 2 m from the connection at the source end. Prepare a flat endface to ensure maximum Fresnel reflection. Attach this end to port C.

- Scan the VOA again to obtain the measured input power through port C. Return the VOA to minimum power.
- The power values are normally reported in dBm.

II.5.4 Calculation and interpretation of results

The data analysis depends on the SBS power rating definition chosen. For definition A, the data must be smoothed by fitting to a high-order polynomial. Definition B requires no fit, but accuracy can be enhanced by a low order polynomial fit (linear interpolation is acceptable). The manner of deployment can affect the measured results. In either case, after the SBS power rating is determined, add 0.14 dB to take into account the Fresnel reflection associated with the end of the fibre.

II.5.4.1 Data analysis using definition A

The smoothing required by method A can be accomplished by truncating the data and using a high-order polynomial (sixth order or higher) or by using a spline fit (fourth order or higher). For options 1 and 2, the fitting is normally done in dBm and then the results are converted to milliwatt power second derivatives using calculus. Using the high-order polynomial fit requires truncating the data outside the input power region where the reflected power rises rapidly. The spline fit requires substantial data be taken outside of this region.

Figure II.5 shows typical data for reflected and transmitted power at different input power levels (data taken at 0.1 dB intervals in input power). The symbols and solid lines show the measured and fitting results, respectively. The notations mark the input powers at which the second derivative of the reflected power is at a maximum (option 1), the second derivative of the transmitted power is minimum (option 2) and the first derivative of the reflected power is maximum (option 3). The SBS power rating obtained from definition B is shown for comparison. Figure II.6 shows the second derivative of the reflected power (option 1) with maximal acceleration power denoted by the dash-dotted line. Figure II.7 shows the second derivative of the transmitted power (option 2) with the minimal acceleration power denoted by the dash-dotted line. Figure II.8 shows the first derivative of the reflected power (option 3) with the maximal rate of increase power denoted by the dash-dotted line. In this case, the knot spacing for the fourth order spline fit was 0.66 dB.

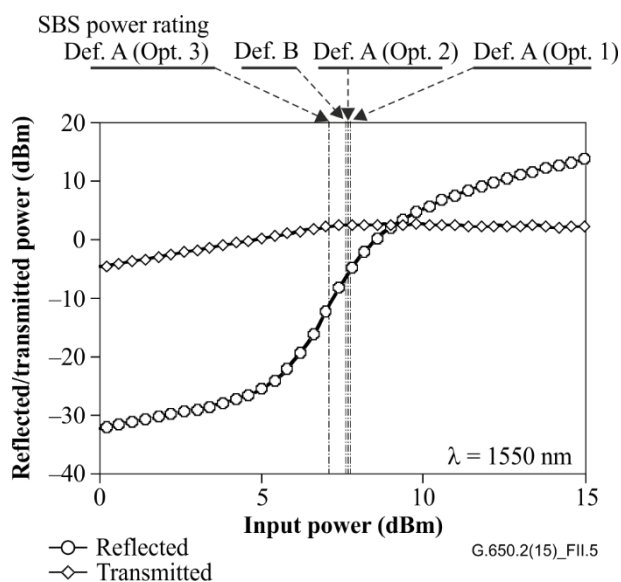


Figure II.5 – Example of reflected and transmitted power

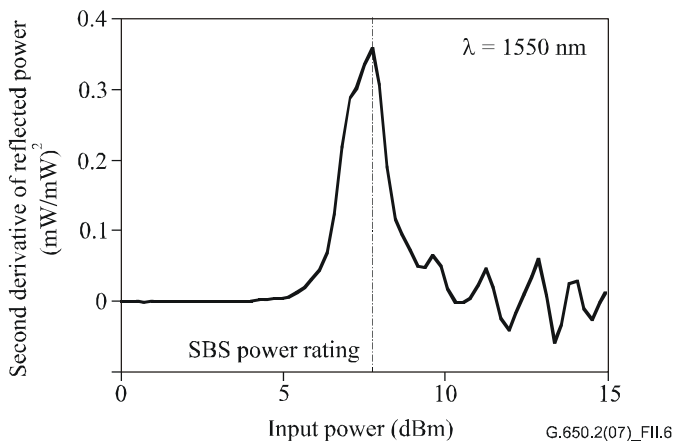


Figure II.6 – Example of the second derivative of reflected power in milliwatts (option 1 of definition A)

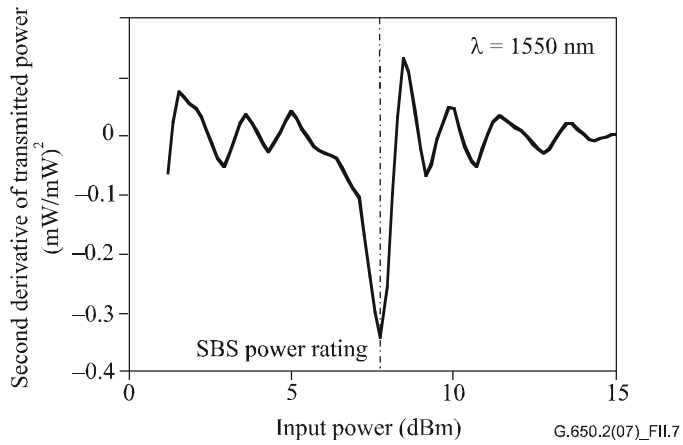


Figure II.7 – Example of the second derivative of transmitted power in milliwatts (option 2 of definition A)

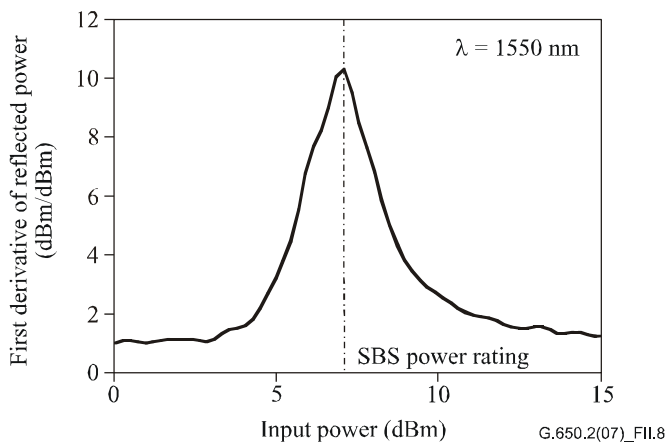


Figure II.8 – Example of first derivative of reflected power in dBm (option 3 of definition A)

II.5.4.2 Data analysis using definition B

Figure II.9 shows application of definition B. The intersection of the reflected power data curve with a line drawn for reflected power of 4% of input power gives the SBS power rating. A comparison of the SBS power rating found from definition B with those of definition A is given in Figure II.5.

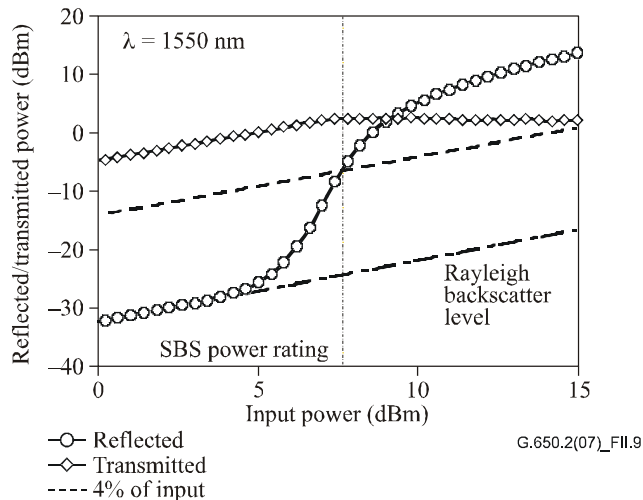


Figure II.9 – Example of 4% of input power (definition B)

II.5.4.3 Uncertainty in measurement and calculation of SBS power rating

A properly implemented measurement can allow a repeatability of the SBS power rating within approximately ± 0.1 dB. There can be differences between the different definitions of the order of 0.5 dB. Non-SBS related reflections, due to improper fibre termination, can cause elevated levels of backscatter leading to incorrect results. There are trade-offs between the definitions that place different priorities on certain details of the implementation:

- Definition A requires fitting a high-order polynomial for differentiation. The choice of algorithm to perform this fit can cause different results (of the order of the measurement repeatability). Measurement noise has a more pronounced effect on the result using this definition than definition B. Best results, particularly for options 1 and 2, are obtained when the input power level is sufficient to see a roll-off in the reflected power (on a dB/dB scale) in the high-power regime.
- Definition B requires an absolute calibration of the splitter or circulator used to capture the reflected light. This definition is less sensitive to noise since a simpler fitting model can be used to interpolate the SBS power rating. Because of the roughly straight-line behaviour of the reflected power near the SBS power rating, estimation can be made of the rating even for data sets where the input power is insufficient to exceed the rating value.

II.5.4.4 Conversion of dBm derivatives to milliwatt derivatives

Transformations to be used with definition A, options 1 and 2. After the dBm/dBm data are fitted to a polynomial, define x as the input power (dBm) and $f(x)$ as the transmitted or reflected power (dBm). Define y as the input power, in milliwatts, and $g(y)$ as the response, in milliwatts.

$$\frac{dg(y)}{dy} = \frac{df(x)}{dx} \exp\left[\frac{\ln 10}{10}(f(x)-x)\right] \quad (\text{II-6})$$

$$\frac{d^2g(y)}{dy^2} = \left\{ \frac{df(x)}{dx} \left[\frac{df(x)}{dx} - 1 \right] + \frac{10}{\ln 10} \frac{d^2f(x)}{dx^2} \right\} \exp\left\{ \frac{\ln 10}{10}[f(x)-2x] \right\} \quad (\text{II-7})$$

The relationship of dBm to milliwatt power is:

$$dBm = 10 \log_{10}(mW) \quad (\text{II-8})$$

II.5.4.5 Length normalization

The SBS power rating value varies with length. For some applications, the value must be reported for the particular length that is measured or used.

For a comparison of fibres of different lengths, it is recommended that the measured value be normalized to a standardized length (L_{STD}). For access networks, a value of 20 km is recommended.

Length normalization can be done with either of two approaches: one based on the classical formula of Equation II-9 or one which is more exact but more complex (Equation II-13). There is a slight (0.1 dB to 0.2 dB) bias associated with the classical formula.

II.5.4.5.1 Classical formula

Classically SBS power rating has been described as Equation II-9 [b-Smith, 1972], and the classical formula has been used by many researchers because it makes the explanatory mathematics easier.

$$P_{\text{CR}} = 21 \frac{KA_{\text{eff}}}{g_B^{\text{eff}} L_{\text{eff}}} \left(1 + \frac{\Delta v}{\Delta v_B} \right) \text{ (W)} \quad (\text{II-9})$$

where:

g_B^{eff} is the effective Brillouin gain coefficient

K is a constant between 1 and 2 reflecting the polarization state

A_{eff} is the effective area

L_{eff} is the effective length

Δv is the source linewidth

Δv_B is the Brillouin linewidth (~ 20 MHz)

$$L_{\text{eff}} = \frac{1 - \exp(-\alpha L)}{\alpha} \quad (\text{II-10})$$

$$\alpha = \frac{\ln 10}{10} a \quad (\text{II-11})$$

where:

L is the measured length, in kilometres

a is the attenuation coefficient, in decibels per kilometre

Define $SBS_T(L)$ as the measured SBS power rating (dBm) at length L , in kilometres, and $SBS_T(L_{\text{STD}})$ as the normalized value for the standard length, L_{STD} . Then from Equation II-9:

$$SBS_T(L_{\text{STD}}) = SBS_T(L) + 10 \log_{10} \left[\frac{1 - \exp(-\alpha L)}{1 - \exp(-\alpha L_{\text{STD}})} \right] \quad (\text{II-12})$$

where α is defined as in Equation II-11.

II.5.4.5.2 A more exact formula

This is extracted from [b-Kobyakov 2002]. A two-stage solution of a non-linear equation is used. The formula is based on Equation II-13:

$$P_{\text{th}}(L) = \frac{\alpha A_{\text{eff}}^{\text{ac}}}{g_B} \gamma_B(L) \text{ (W)} \quad (\text{II-13})$$

where:

$A_{\text{eff}}^{\text{ac}}$ is the acousto-optic effective area

α is as defined in Equation II-11

$\gamma_B(L)$ is a dimensionless parameter depending on length

$$g_B = \frac{\tilde{g}_B(v)}{K(1 + \Delta v / \Delta v_B)}$$

where:

K , Δv , and Δv_B are as defined in Equation II-9

$\tilde{g}_B(v)$ is the Brillouin gain coefficient, in metres per watt)

The ratio, $\gamma_B(L)/P_{\text{th}}(L)$, is a constant independent of length

The dimensionless parameter, $\gamma_B(L)$ is solved using the following non-linear equation and the measured SBS power rating, P_{th} :

$$\frac{\exp\{-\gamma_B(L)[1 - \exp(-\alpha L)]\}}{\left[\frac{1}{\gamma_B(L)} + \exp(-\alpha L)\right]} \gamma_B^{3/2}(L) \sqrt{1 - \exp(-\alpha L)} = C' \frac{\gamma_B(L)}{P_{\text{th}}(L)} \quad (\text{II-14})$$

where:

$$C' = \sqrt{\pi k T} \frac{v_s}{v_a} \Delta v_B \cong 2.612 \times 10^{-9} \quad (\text{II-15})$$

k is the Boltzmann constant ($1.380\,658 \times 10^{-23}$)

T is the temperature (298°K at room temperature)

v_s is the signal frequency (193.4 THz for 1 550 nm)

v_a is the frequency difference between the Stokes wave and the signal (10.8 GHz)

Given the ratio, $\gamma_B(L)/P_{\text{th}}(L)$, Equation II-14 is reapplied using L_{STD} to determine $\gamma_B(L_{\text{STD}})$. The value of $P_{\text{th}}(L_{\text{STD}})$ follows immediately from the constant ratio. [It must then be converted to dBm for reporting purposes.]

The value of C' can be varied by plus or minus an order of magnitude from the value presented in Equation II-15. The calculated values of the SBS power rating vary of the order ± 0.01 dB as a result of varying the value of C' in this way.

II.5.4.6 Attenuation normalization

The SBS power rating value varies with attenuation. For some applications, the value must be reported for the particular attenuation that is measured or used.

For a comparison of fibres of different attenuation, it is recommended that the measured value be normalized to a standardized attenuation. For a standard attenuation, a value of 0.2 dB/km is recommended.

Define $SBS_T(\alpha)$ as the measured SBS power rating (dBm) at attenuation α , in decibels per kilometre, and $SBS_T(\alpha_{STD})$ as the normalized value for the standard attenuation, α_{STD} . Then from Equation II-9:

$$SBS_T(\alpha_{STD}) = SBS_T(\alpha) + 10 \log_{10} \left[\frac{\alpha_{STD}}{\alpha} \frac{1 - \exp(-\alpha L)}{1 - \exp(-\alpha_{STD} L)} \right] \quad (\text{II-16})$$

where α is defined as in Equation II-11.

II.5.5 Documentation

The following information is reported:

- wavelength and source linewidth.
- Definition (A, B).
- For definition A, implementation option, details of mathematical fit.
- The SBS power rating value.
- For length normalized values, the normalization length and normalizing formula used.
- For attenuation normalized values, the normalization attenuation.

II.6 Other effects

For a description of other optical non-linear effects (four-wave mixing, modulation instability, self-phase modulation, cross-phase modulation, solitons and stimulated Raman scattering), see Appendix II of [[b-ITU-T G.663](#)].

Appendix III

Test methods for effective area (A_{eff})

(This appendix does not form an integral part of this Recommendation.)

III.1 The far-field scan (FFS) technique

III.1.1 General

The effective area (A_{eff}) of single-mode optical fibres is determined by the far-field scan (FFS) technique.

III.1.2 Test apparatus

A schematic diagram of the test set-up for far-field scan (FFS) is shown in Figure III.1.

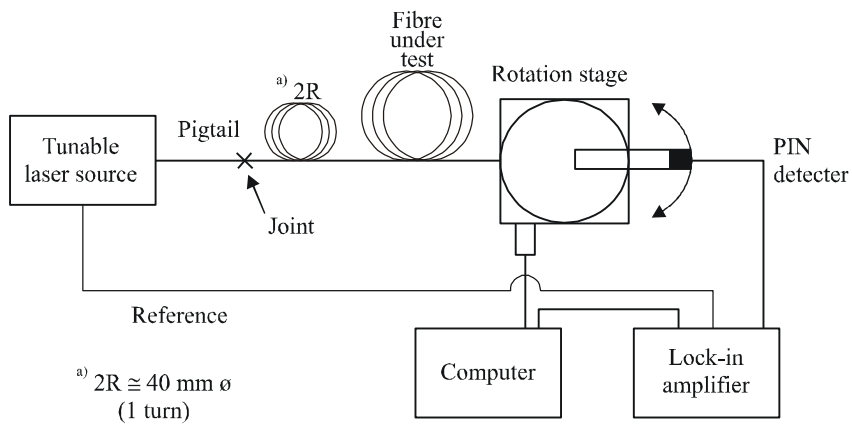


Figure III.1 – Typical arrangement of far-field scan (FFS) set-up

- III.1.2.1 **Light source** (as in clause 5.1.1.2.1 of [[b-ITU-T G.650.1](#)]).
- III.1.2.2 **Modulation** (as in clause 5.1.1.2.2 of [[b-ITU-T G.650.1](#)]).
- III.1.2.3 **Launching conditions** (as in clause 5.1.1.2.3 of [[b-ITU-T G.650.1](#)]).
- III.1.2.4 **Cladding mode stripper** (as in clause 5.1.1.2.4 of [[b-ITU-T G.650.1](#)]).
- III.1.3.5 **Specimen** (as in clause 5.1.1.2.5 of [[b-ITU-T G.650.1](#)]).
- III.1.2.6 **Scan apparatus** (as in clause 5.1.1.2.6 of [[b-ITU-T G.650.1](#)]).
- III.1.2.7 **Detector** (as in clause 5.1.1.2.7 of [[b-ITU-T G.650.1](#)]).
- III.1.2.8 **Amplifier** (as in clause 5.1.1.2.8 of [[b-ITU-T G.650.1](#)]).
- III.1.2.9 **Data acquisition** (as in clause 5.1.1.2.9 of [[b-ITU-T G.650.1](#)]).

III.1.3 Measurement procedure

The launch end of the fibre shall be aligned with the launch beam, and the output end of the fibre shall be aligned to the appropriate output device.

The effective area (A_{eff}) is computed from Equation III-1.

III.1.3.1 Equipment calibration

For equipment calibration, the magnification of the magnifying optics shall be measured by scanning the length of a specimen whose dimensions are already known with suitable accuracy. This magnification shall be recorded.

III.1.3.2 Calculations

III.1.3.2.1 Equations and figures for effective area (A_{eff}) calculation

- 1) *Fold the far-field radiation power data*

Let $P(\theta_i)$ be the measured power as a function of angular position, θ_i (radians). The folded power curve, $P_f(\theta_i)$, for $0 \leq \theta_i \leq \theta_{\max}$ is:

$$P_f(\theta_i) = \frac{P(\theta_i) + P(-\theta_i)}{2} \quad (\text{III-1})$$

- 2) *Compute the near-field intensity pattern*

Use an appropriate numerical integration method to compute the integrals of Equation III-1. Equation III-2 is an example. Any other integration method shall be at least as accurate.

Calculate the near-field values for a range of radii, r_j , values ranging from zero to a value large enough that the computed intensity at the maximum radius is less than 0.01% of the maximum intensity.

$$I(r_j) = \left\{ \sum_{i=0}^n \sqrt{P_f(\theta_i)} J_0 \left[\frac{2\pi r_j \sin(\theta_i)}{\lambda} \right] \sin(2\theta_i) \Delta\theta \right\}^2 \quad (\text{III-2})$$

where $\Delta\theta = \theta_1 - \theta_0$ and J_0 is the Bessel function of order 0.

NOTE – The square root of the power, $P_f(\theta_i)$, in Equation III-2 is taken in order to calculate the far-field amplitude from the measured power values. For some very large values of θ_i , it might be possible that after crossing zero the amplitude must adopt the negative root. One way to avoid this difficulty is to choose θ_{\max} low enough to ensure that the measured power for all lower angles is greater than the measurement uncertainty.

- 3) *Compute the integrals of Equation III-2*

Use an appropriate numerical integration method to compute the integrals of Equation III-2. Equation III-3 is an example. Any other integration method shall be at least as accurate.

$$T = \left[\sum_{j=0}^m I(r_j) r_j \Delta r \right]^2 \quad (\text{III-3})$$

$$B = \sum_{j=0}^m I^2(r_j) r_j \Delta r \quad (\text{III-4})$$

where $\Delta r = r_1 - r_0$, and m is the number of positions calculated from Equation III-2.

- 4) *Complete the calculation*

$$A_{\text{eff}} = \frac{2\pi T}{B} \quad (\text{III-5})$$

An example of measured far-field power data is shown in Figure III.2.

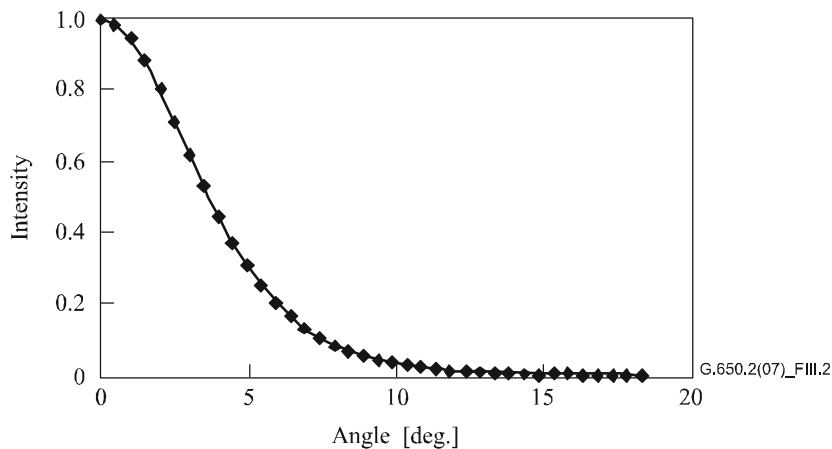


Figure III.2 – Example of measured FFP data

III.1.4 Presentation of the results

The following details shall be presented:

- a) Test set-up arrangement, dynamic range of the measurement system, processing algorithms, and a description of the aperture assembly used (including the numerical aperture).
- b) Launching conditions.
- c) Wavelength and spectral linewidth FWHM of the source.
- d) Fibre identification and length.
- e) Type of cladding mode stripper.
- f) Type and dimensions of the detector.
- g) Temperature of the sample and environmental conditions (when necessary).
- h) Indication of the accuracy and repeatability.
- i) Effective area (A_{eff}).
- j) Plot of $A_{\text{eff}} (\lambda)$ (if required).

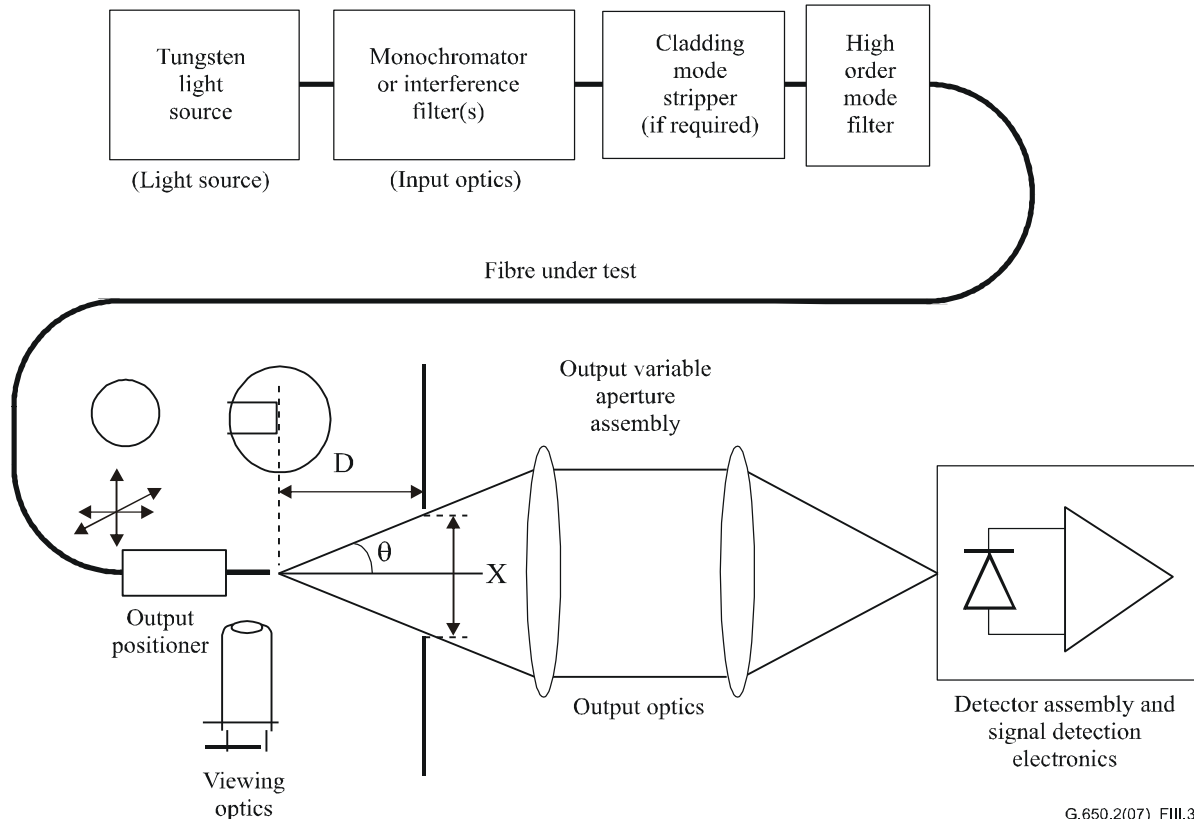
III.2 The variable aperture (VA) technique

III.2.1 General

The effective area (A_{eff}) of SMFs is determined by the variable aperture in the far-field (VA) measurement technique.

III.2.2 Test apparatus

A schematic diagram of the test set-up for VA technique is shown in Figure III.3.



G.650.2(07)_FIII.3

Figure III.3 – Typical arrangement of the variable aperture (VA) technique set-up

- III.2.2.1 Light source** (as in clause 5.1.1.2.1 of [[b-ITU-T G.650.1](#)]).
- III.2.2.2 Modulation** (as in clause 5.1.1.2.2 of [[b-ITU-T G.650.1](#)]).
- III.2.2.3 Launching conditions** (as in clause 5.1.1.2.3 of [[b-ITU-T G.650.1](#)]).
- III.2.2.4 Cladding mode stripper** (as in clause 5.1.1.2.4 of [[b-ITU-T G.650.1](#)]).
- III.2.2.5 Specimen** (as in clause 5.1.1.2.5 of [[b-ITU-T G.650.1](#)]).
- III.2.2.6 Aperture apparatus**

A mechanism covering at least 12 apertures spanning the half-angle range of numerical apertures from 0.02 to 0.25 (0.4 for fibres covered by [[b-ITU-T G.653](#)]) should be used. Light transmitted by the aperture is collected and focused onto the detector.

NOTE – The numerical aperture of the collecting optics must be large enough not to affect the measurement results.

III.2.2.7 Output variable aperture assembly

A device consisting of round transmitting apertures of various sizes (such as an aperture wheel), shall be placed a distance D of at least $100 w^2/\lambda$ from the fibre end, and is used to vary the power collected from the fibre output pattern. Typically 12 to 20 apertures are used and are located about 20–50 mm away from the fibre end. The maximum numerical aperture of the test set shall be equal to 0.40. Means of centring the apertures with respect to the pattern shall be employed to decrease sensitivity to fibre end-angle.

As part of the equipment set-up (as shown in Figure III.4), carefully measure and record the longitudinal distance D between the fibre output end position and the aperture plane and the diameters X_i of each aperture. Determine the half-angle subtended by each aperture in the wheel and record these θ_i , ($i = 1 \dots n$ in order of increasing aperture size) values for future calculation. These values are independent of test wavelength.

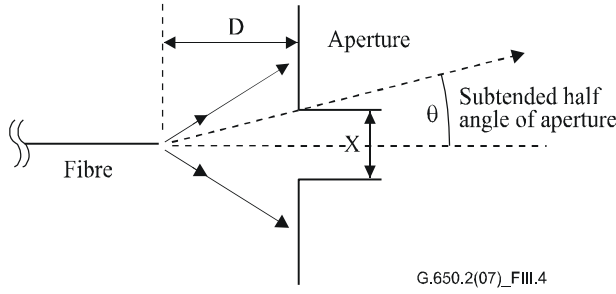


Figure III.4 – Aperture apparatus set-up

III.2.2.8 Detector (as in clause 5.1.1.2.7 of [[b-ITU-T G.650.1](#)]).

III.2.2.9 Amplifier (as in clause 5.1.1.2.8 of [[b-ITU-T G.650.1](#)]).

III.2.2.10 Data acquisition (as in clause 5.1.1.2.9 of [[b-ITU-T G.650.1](#)]).

III.2.3 Measurement procedure

The launch end of the fibre shall be aligned with the launch beam, and the output end of the fibre shall be aligned to the appropriate output device.

The effective area (A_{eff}) is computed from Equations III-6 to III-10.

III.2.3.1 Equipment calibration

For equipment calibration, the magnification of the magnifying optics shall be measured by scanning the length of a specimen whose dimensions are already known with suitable accuracy. This magnification shall be recorded.

III.2.3.2 Calculations

III.2.3.2.1 Equations and figures for effective area (A_{eff}) calculation

The variable aperture (VA) technique measures the total normalized power $f(\theta)$ passing through a given aperture as shown in Figure III.3 subtending a far-field half-angle θ at the fibre. These power values are equivalent to an integration of the normalized far-field power distribution $F^2(\theta)$. This is represented by Equation III-6.

$$f(\theta) = \int_0^\theta F^2(\theta) \sin(\theta) d\theta \quad (\text{III-6})$$

A plot of normalized power transmitted through the apertures as a function of half-angle θ is shown in Figure III.5.

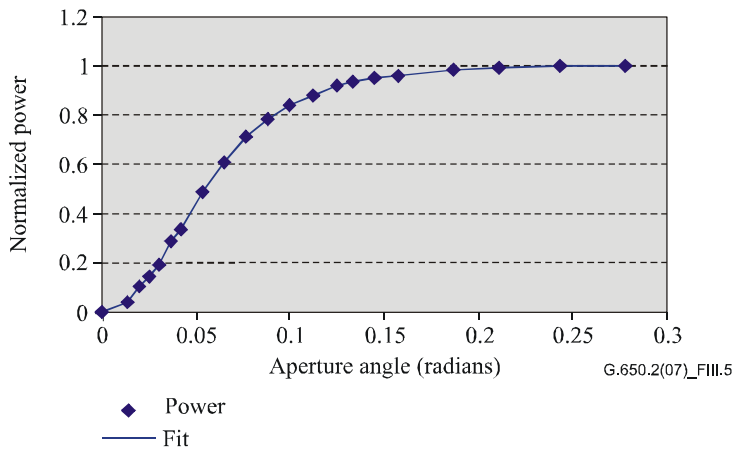


Figure III.5 – Plot of measured VA data

The far-field aperture data, given by Equation III-7, is fitted to a smooth function such as the quartic function:

$$f(\theta) = A\theta^4 + B\theta^3 + C\theta^2 + D\theta^1 + E \quad (\text{III-7})$$

Effective area, A_{eff} , is calculated from the near-field power distribution $I(r)$ given as a function of radius r . To calculate this, one must first differentiate the integrated power data, $f(\theta)$, to give the far-field power distribution $F^2(\theta)$,

$$F^2(\theta) = \frac{df(\theta)}{d(\theta)} \cdot \frac{1}{\sin \theta} \quad (\text{III-8})$$

A plot of this calculated FFP distribution is shown in Figure III.6.

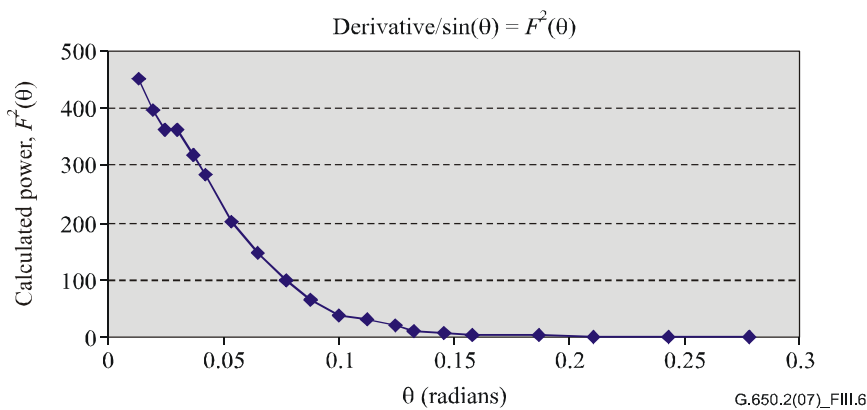


Figure III.6 – Plot of FFP distribution

From the far-field power distribution $F^2(\theta)$, it is then possible to calculate the near-field power distribution $I(r)$ as a function of radius r , using the inverse Hankel transform as follows:

$$I(r) = \left[\int_0^\infty \sqrt{F^2(\theta)} J_0\left(\frac{2\pi r \sin(\theta)}{\lambda}\right) \sin(2\theta) d\theta \right]^2 \quad (\text{III-9})$$

A plot of this calculated near-field distribution $I(r)$ as a function of radius r is shown in Figure III.7.

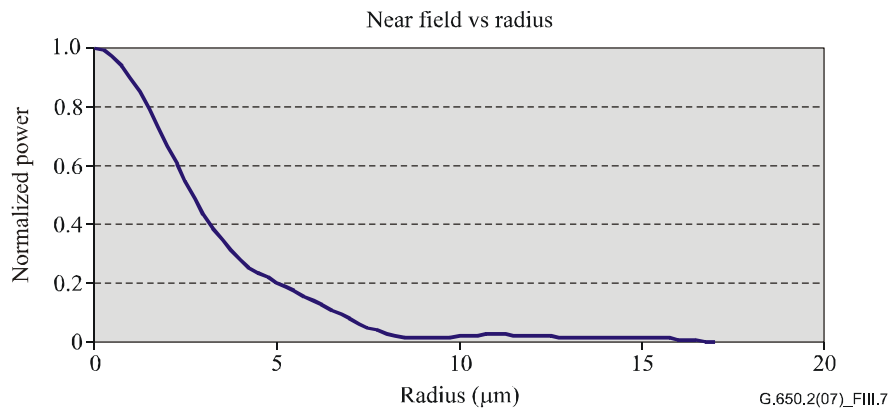


Figure III.7 – Plot of NFP distribution

Effective area, A_{eff} , is then calculated from the near-field distribution $I(r)$ using Equation III-10.

$$A_{\text{eff}} = 2\pi \cdot \frac{\left[\int_0^{\infty} I(r) \cdot r dr \right]^2}{\int_0^{\infty} I(r)^2 \cdot r dr} \quad (\text{III-10})$$

III.2.4 Presentation of the results

The following details shall be presented:

- a) Test set-up arrangement, dynamic range of the measurement system, processing algorithms, and a description of the aperture assembly used (including the numerical aperture).
- b) Launching conditions.
- c) Wavelength and spectral linewidth FWHM of the source.
- d) Fibre identification and length.
- e) Type of cladding mode stripper.
- f) Type and dimensions of the detector.
- g) Temperature of the sample and environmental conditions (when necessary).
- h) Indication of the accuracy and repeatability.
- i) Effective area (A_{eff}).
- j) Plot of $A_{\text{eff}}(\lambda)$ (if required).

III.3 The near-field scan (NFS) technique

III.3.1 General

The effective area (A_{eff}) of single-mode fibres is determined by the near-field scan (NFS) measurement technique.

III.3.2 Test apparatus

- III.3.2.1 Light source** (as in clause 5.1.1.2.1 of [[b-ITU-T G.650.1](#)]).
- III.3.2.2 Modulation** (as in clause 5.1.1.2.2 of [[b-ITU-T G.650.1](#)]).
- III.3.2.3 Launching conditions** (as in clause 5.1.1.2.3 of [[b-ITU-T G.650.1](#)]).
- III.3.2.4 Cladding mode stripper** (as in clause 5.1.1.2.4 of [[b-ITU-T G.650.1](#)]).

- III.3.2.5 Specimen** (as in clause 5.1.1.2.5 of [[b-ITU-T G.650.1](#)]).
- III.3.2.6 Scan apparatus** (as in clause 5.1.1.2.6 of [[b-ITU-T G.650.1](#)]).
- III.3.2.7 Detector** (as in clause 5.1.1.2.7 of [[b-ITU-T G.650.1](#)]).
- III.3.2.8 Amplifier** (as in clause 5.1.1.2.8 of [[b-ITU-T G.650.1](#)]).
- III.3.2.9 Data acquisition** (as in clause 5.1.1.2.9 of [[b-ITU-T G.650.1](#)]).

III.3.3 Measurement procedure

The launch end of the fibre shall be aligned with the launch beam, and the output end of the fibre shall be aligned to the appropriate output device.

The effective area (A_{eff}) is computed from Equations III-11 to III-15.

III.3.3.1 Equipment calibration

For equipment calibration, the magnification of the magnifying optics shall be measured by scanning the length of a specimen whose dimensions are already known with suitable accuracy. This magnification shall be recorded.

III.3.3.2 Calculations

III.3.3.2.1 Equations and figures for effective area (A_{eff}) calculation

1) *Calculate the centroid*

For a given cross-section of the NFP that is of maximum extent, with position values given by r and intensity values as $I(r_i)$, the centroid position, r_c , is given as:

$$r_c = \frac{\sum r_i I(r_j)}{\sum I(r_i)} \quad (\text{III-11})$$

2) *Fold the intensity profile*

Rank the position and intensity data around the position r_c so that positions above have subscript values greater than zero and positions below have subscript values less than zero. The maximum subscript is given as n . The folded intensity profile is:

$$I_f(r_i) = [I(r_i) + I(r_{-i})]/2 \quad (\text{III-12})$$

3) *Compute the integrals from Equation III-12*

Use an appropriate numerical integration method to compute the integrals of Equation III-12. The following is an example. Any other integration method shall be at least as accurate.

$$T = \left[\sum_0^m I(r_j) r_j \Delta r \right]^2 \quad (\text{III-13})$$

$$B = \sum_0^m I^2(r_j) r_j \Delta r \quad (\text{III-14})$$

where $\Delta r = r_1 - r_0$

4) *Complete the calculation*

$$A_{\text{eff}} = \frac{2\pi T}{B} \quad (\text{III-15})$$

An example of a calculated NFP is shown in Figure III.7.

III.3.4 Presentation of the results

The following details shall be presented:

- a) Test set-up arrangement, dynamic range of the measurement system, processing algorithms, and a description of the aperture assembly used (including the numerical aperture).
- b) Launching conditions.
- c) Wavelength and spectral linewidth FWHM of the source.
- d) Fibre identification and length.
- e) Type of cladding mode stripper.
- f) Type and dimensions of the detector.
- g) Temperature of the sample and environmental conditions (when necessary).
- h) Indication of the accuracy and repeatability.
- i) Effective area (A_{eff}).
- j) Plot of $A_{\text{eff}}(\lambda)$ (if required).

Appendix IV

Information on polarization mode dispersion statistics

(This appendix does not form an integral part of this Recommendation.)

This appendix is provided to summarize some of the statistical calculations for PMD. [b-IEC/TR 61282-3] documents the calculations and theory more completely.

NOTE – Other calculation methods are allowed and defined in [b-IEC/TR 61282-3]. The Monte Carlo method is given here because it is the easiest to describe and uses the fewest assumptions.

IV.1 Introduction

PMD is a statistical attribute that, for a given fibre, is defined as the average of measured DGD values across a range of wavelengths. Since the DGD values are random across time and wavelength, there is a theoretical lower limit to achievable reproducibility of the reported PMD value of approximately $\pm 15\%$. This feature implies that it is not appropriate to select individual fibres or cables to a specification that is tighter than the capability of the process. Such selections are often appropriate for deterministic attributes, such as attenuation, but are not generally appropriate for PMD. This means that a specification on the overall process distribution is most reasonable.

A second consideration regarding the functionality of PMD is that system impairment at a given time and wavelength is controlled by the DGD value, which varies statistically around the PMD value. If the PMD value for a particular cabled fibre is given, the probability that DGD exceeds a given value can be calculated. It is clear, however, that application of these formulae to a maximum specified value will yield a very inaccurate view of the actual system performance. A statistical specification on PMD, however, can lead to a statistical boundary on the DGD values for the population as a whole. This boundary, defined in terms of probability, leads to a value for use in system design that is approximately 20% lower in DGD value and two orders of magnitude less in probability than the values that would be obtained without a statistical specification.

From the first consideration, it is desirable to define a single statistical metric for the distribution of the PMD values that are measured on optical fibre cables. The metric, therefore, must incorporate both aspects of process mean and process variability. An upper confidence limit at some probability level is such a metric.

It is known that the PMD coefficient of a set of concatenated cables can be estimated by the computation of the quadrature average of the PMD coefficients of the individual cables. To give the upper confidence limit metric more meaning in terms of application, the upper bound for a concatenated link of 20 cables is computed. This number of cable sections is smaller than that used in most links, but is large enough to be meaningful in terms of projecting DGD distributions for concatenated links. A probability value of 0.01% is also standardized, partially on the basis of obtaining equivalence with the probability that DGD exceeds a bound, which is required to be very low. The upper confidence limit is named PMD_Q , or link design value and this specification type is known as method 1.

The probability limit for DGD is set at 6.5×10^{-8} based on various system considerations including the presence of other PMD-generating components that may be in the links. [b-IEC/TR 61282-3] describes a method of determining a maximum (defined in terms of probability), so that if a distribution passes the method 1 requirement, the DGD across links comprised of only optical fibre cable will exceed the maximum DGD with a probability less than 6.5×10^{-8} . The DGD_{\max} value is established for a broad range of distribution shapes. This DGD_{\max} method of specifying the PMD distribution of optical fibre cables is known as method 2. Methods of combining the method 2 parameters with those of other optical components are given in [b-IEC/TR 61282-3].

Method 1 is a metric that is based on what is measured and is, therefore, somewhat more straightforward for use in trade and commerce as a normative requirement. Method 2 is a means of extrapolating the implications for system design and is, therefore, included as information for system design.

IV.2 Data collection

The calculations are done with PMD values that are representative of a given cable construction and manufacturing time period. Typically at least 100 values are required. The sample is normally taken on different production cables and different fibre locations within the cables.

The cable distribution can be augmented by measurements of uncabled fibre provided that a stable relationship between uncabled fibre and cable values has been demonstrated for a given construction. One means of such augmentation is to generate several possible cable values from the value of each uncabled fibre. These different values should be selected randomly to represent both the usual relationship and the variability that follows from, for example, measurement reproducibility. Because the range of variations includes reproducibility error, this method of estimating the distribution of cable PMD values can lead to over-estimation of PMD_Q .

The length of the samples measured could seem to have implications on the method 2 deductions. This has been studied with the following conclusions. The method 2 implications remain valid for any link less than 400 km provided that either:

- the installed cable sections are less than 10 km; or
- the measured lengths are less than 10 km.

IV.3 Calculation of PMD_Q (Monte Carlo)

The measured PMD coefficient values are represented by x_i , with i ranging from 1 to N , the number of measurements. These values will be used to generate 100 000 concatenated link PMD coefficient values, each computed with the quadrature average of 20 individual cable values that are randomly selected from the sample population.

NOTE – When $N = 100$, there are 5.3×10^{20} possible link values.

For each link value computation, select 20 random numbers between 1 and N . Select these values and assign them a subscript, k . The link PMD coefficient, y , is calculated as:

$$y = \left(\frac{1}{20} \sum_{k=1}^{20} x_k^2 \right)^{1/2} \quad (\text{IV-1})$$

Collect the 100 000 values of y into a high density histogram as they are being computed. When this computation is complete, calculate the cumulative probability function from the histogram and determine the PMD value associated with the 99.99% level. Report this value as PMD_Q . If the computed PMD_Q is less than the specified value [$0.5 \text{ ps/km}^{\sqrt{2}}$], the distribution passes method 1.

IV.4 Calculation for DGD_{\max} (Monte Carlo)

This calculation builds on that of the calculation for PMD_Q . In this calculation, a value of DGD_{\max} is predefined (at 25 ps) and a probability of exceeding this value, P_F , is calculated. If the computed probability is less than the specified value (6.5×10^{-8}), the distribution passes method 2.

Before beginning the Monte Carlo, calculate the PMD coefficient limit, P_{\max} , as:

$$P_{\max} = \frac{\text{DGD}_{\max}}{\sqrt{L_{\text{ref}}}} = \frac{25}{20} = 1.25$$

For each subsequent pair of 20 cable link concatenation values, y_j and y_{j+1} , a 40-cable concatenation value, z_j , is generated as:

$$z_j = \left(\frac{y_j^2 + y_{j+1}^2}{2} \right)^{1/2} \quad (\text{IV-2})$$

NOTE – This yields 50 000 values of z_j , an adequate number.

Calculate the probability of exceeding DGD_{\max} on the j th concatenation of 40 links, p_j , as:

$$p_j = 1 - \int_0^{P_{\max}/z_j} 2 \left(\frac{4}{\pi} \right)^{3/2} \frac{t^2}{\Gamma(3/2)} \exp \left[-\frac{4}{\pi} t^2 \right] dt \quad (\text{IV-3})$$

Microsoft Excel™ defines a function that can compute p_j , GAMMADIST (x, alpha, beta, cumulative). The call to this function should be:

$$PJ = 1 - \text{GAMMADIST}(4 \times PMAX \times PMAX / (PI() \times ZI \times ZI), 1.5, 1, \text{TRUE}) \quad (\text{IV-4})$$

The probability of exceeding DGD_{\max} , P_F , is given as:

$$P_F = \frac{1}{50\,000} \sum_j p_j \quad (\text{IV-5})$$

If P_F is less than the specified value, the distribution passes method 2.

Bibliography

- [b-ITU-T G.650.1] Recommendation ITU-T G.650.1 (2010), *Definitions and test methods for linear, deterministic attributes of single-mode fibre and cable.*
- [b-ITU-T G.651.1] Recommendation ITU-T G.651.1 (2007), *Characteristics of a 50/125 µm multimode graded index optical fibre cable for the optical access network.*
- [b-ITU-T G.652] Recommendation ITU-T G.652 (2009), *Characteristics of a single-mode optical fibre and cable.*
- [b-ITU-T G.653] Recommendation ITU-T G.653 (2010), *Characteristics of a dispersion-shifted, single-mode optical fibre and cable.*
- [b-ITU-T G.654] Recommendation ITU-T G.654 (2012), *Characteristics of a cut-off shifted single-mode optical fibre and cable.*
- [b-ITU-T G.655] Recommendation ITU-T G.655 (2009), *Characteristics of a non-zero dispersion-shifted single-mode optical fibre and cable.*
- [b-ITU-T G.656] Recommendation ITU-T G.656 (2010), *Characteristics of a fibre and cable with non-zero dispersion for wideband optical transport.*
- [b-ITU-T G.657] Recommendation ITU-T G.657 (2012), *Characteristics of a bending-loss insensitive single-mode optical fibre and cable for the access network.*
- [b-ITU-T G.663] Recommendation ITU-T G.663 (2011), *Application-related aspects of optical amplifier devices and subsystems.*
- [b-ITU-T G.666] Recommendation ITU-T G.666 (2011), *Characteristics of polarization mode dispersion compensators and of receivers that compensate for polarization mode dispersion.*
- [b-ITU-T G.671] Recommendation ITU-T G.671 (2012), *Transmission characteristics of optical components and subsystems.*
- [b-IEC/TR 61282-3] IEC/TR 61282-3 (2006), *Fibre optic communication system design guides – Part 3: Calculation of link polarization mode dispersion.*
- [b-IEC/TR 61282-9] IEC/TR 61282-9 (2006), *Fibre optic communication system design guides – Part 9: Guidance on polarization mode dispersion measurements and theory.*
- [b-IEC 61315] IEC 61315 (2005), *Calibration of fibre-optic power meters.*
- [b-Kobyakov 2002] Kobyakov, A., Mehwendale, M., Vasilyev, M., Tsuda, S., Evans, A.F. (2002), Stimulated Brillouin scattering in Raman-pumped fibers: A theoretical approach, *Journal of Lightwave Technology*, **20**, pp. 1635–43.
- [b-Namihira 1994] Namihira, Y. (1994), Relationship between nonlinear effective area and mode field diameter for dispersion shifted fibres, *Electronics Letters*, **30**, pp. 262–264.
- [b-Press 1992] Press, W.H, Flannery, B.P, Teukolsky, S.A, Vetterling, W.T. (1992), *Numerical recipes in C: The art of scientific computing*, 2nd edition, Cambridge University Press.
- [b-Smith, 1972] Smith, R.G. (1972), Optical power handling capacity of low loss optical fibers as determined by stimulated Raman and Brillouin scattering, *Applied Optics*, **11**, pp. 2489–94.

SERIES OF ITU-T RECOMMENDATIONS

- Series A Organization of the work of ITU-T
- Series D General tariff principles
- Series E Overall network operation, telephone service, service operation and human factors
- Series F Non-telephone telecommunication services
- Series G Transmission systems and media, digital systems and networks**
- Series H Audiovisual and multimedia systems
- Series I Integrated services digital network
- Series J Cable networks and transmission of television, sound programme and other multimedia signals
- Series K Protection against interference
- Series L Environment and ICTs, climate change, e-waste, energy efficiency; construction, installation and protection of cables and other elements of outside plant
- Series M Telecommunication management, including TMN and network maintenance
- Series N Maintenance: international sound programme and television transmission circuits
- Series O Specifications of measuring equipment
- Series P Terminals and subjective and objective assessment methods
- Series Q Switching and signalling
- Series R Telegraph transmission
- Series S Telegraph services terminal equipment
- Series T Terminals for telematic services
- Series U Telegraph switching
- Series V Data communication over the telephone network
- Series X Data networks, open system communications and security
- Series Y Global information infrastructure, Internet protocol aspects and next-generation networks
- Series Z Languages and general software aspects for telecommunication systems